JOURNAL OF GEOPHYSICAL RESEARCH, VOL. 91, NO. D1, PAGES 1117–1135, JANUARY 20, 1986

Concentrations and Uncertainties of Stratospheric Trace Species Inferred from Limb Infrared Monitor of the Stratosphere Data 1. Methodology and Application to OH and HO_2

JACK A. KAYE AND CHARLES H. JACKMAN

Atmospheric Chemistry and Dynamics Branch, NASA Goddard Space Flight Center Greenbelt, Maryland

Zonally averaged limb infrared monitor of the stratosphere data from the Nimbus 7 satellite are used together with an essentially algebraic photochemical equilibrium model to infer concentrations of O_x, HO_x, and NO_x species over most of the stratosphere for the period from March 26, 1979, to April 1, 1979. Since the model is algebraic, sensitivity coefficients (logarithmic partial derivatives of inferred concentrations with respect to model input) may also be calculated. These are combined with estimates of the uncertainty in the model input parameters (concentrations, rate constants, photolysis rates) to give uncertainty factors for the inferred concentrations. Concentrations of OH and HO_2 are calculated and found to compare reasonably well with previous measurements and two-dimensional model calculations. Uncertainties are found, in general, to be largest in the lower stratosphere and to be greater for HO_2 than they are for OH. The method of inference of OH concentration is found to have a great effect on the uncertainty factors calculated for HO_2.

1. INTRODUCTION

With the increasing sophistication of multidimensional chemical models of the stratosphere, the subject of model verification has become an important one. Model verification involves comparison of the results of in situ observations of stratospheric composition with their prediction by the models. The verification process is difficult because of the large amount of uncertainty which enters into it, including uncertainties in the observations; in the models' treatment of chemistry, radiation, and transport; and those arising from the comparison of the spatially and temporally very limited set of measurements with the more highly averaged predictions of the models (uncertainty due to atmospheric variability).

One way of removing this third source of uncertainty is by having a comprehensive data base of stratospheric composition, in which concentrations of species of interest are known over a wide portion of the globe for a long period of time. While such a data base does not exist for many transient species of stratospheric interest (i.e., OH, HO_2, NO, ClO), there has recently been substantial improvement in our knowledge of the distribution of long-lived stratospheric molecules which are not only of great interest in themselves but are also photochemical precursors of shorter-lived species. These data are derived from earth-orbiting satellite-based experiments, most notably three on the Nimbus 7 satellite: limb infrared monitor of the stratosphere (LIMS), stratospheric and mesospheric sounder (SAMS), and solar backscattered ultraviolet (SBUV), which have provided extensive information about concentrations of O_3, NO_2, H_2O, HNO_3 [*Russell et al.*, 1983; *Gille and Russell*, 1984; *Russell*, 1984], N_2O and CH_4 [*Rodgers et al.*, 1984; *Jones and Pyle*, 1984; *Jones*, 1984; *Barnett et al.*, 1985], and O_3 [*McPeters et al.*, 1984], respectively. The solar mesosphere explorer (SME) has also provided information on NO_2 [*Mount et al.*, 1983, 1984] and O_3 [*Thomas et al.*, 1984] in the upper stratosphere as has the stratospheric aerosol and gas experiment (SAGE) experiment on the Applications Explorer Mission 2 (AEM 2) satellite of NASA on O_3 [*Cunnold et al.*, 1984]. Such measurements have not as yet been extended to transient free radical species, such as OH, HO_2, etc., nor have they been extended to longer lived closed-shell molecules such as H_2O_2, HO_2NO_2, and N_2O_5. In addition, there are no satellite-derived data on chlorine-containing compounds.

The comprehensive nature of the LIMS data (latitudinal coverage from 64°S to 84°N from approximately 100 to 1 mbar for the 7-month period from October 25, 1978, to May 29, 1979, at times corresponding roughly to local noon and to local midnight) makes them a valuable starting point for estimation of other stratospheric trace species. The LIMS data contain information about important reservoir molecules for odd oxygen O_x (ozone), odd hydrogen HO_x (water), and odd nitrogen NO_x (nitrogen dioxide, nitric acid). These molecules, being either long-lived themselves or major components in their respective molecular classes, reflect the effects of the actual transport processes operating in the atmosphere. Reactive free radicals and most remaining closed-shell trace species have lifetimes which are substantially shorter than the time scales for transport in much of the stratosphere and are thus in photochemical equilibrium during daytime. In that case, the steady state approximation may be applied, and the expected concentration of trace species not observed by LIMS may be determined. By using a photochemical equilibrium approximation and measured distributions of precursor species we do not need to include any transport parameterizations; in a sense the atmosphere has provided the transport for us by properly distributing the LIMS observables.

Such a method has recently been used by *Pyle et al.* [1983], who used zonally averaged LIMS daytime NO_2 and HNO_3 to derive an estimate of stratospheric OH. Use of this method at altitudes above the 5-mbar pressure level has been called into question because of the fact that LIMS HNO_3 values become unacceptably high above that level [*Jackman et al.*, 1985] (discussion of possible errors in the high-altitude LIMS HNO_3 values has been presented by *Gille et al.* [1984*a*]). *Jackman et al.* [1985] demonstrated a way in which trace species concentrations might be numerically obtained from LIMS observables.

In this work we report the development of an algebraic

Paper number 5D0616.

model for the concentration of O_x, HO_x, and NO_x stratospheric trace species given the concentration of LIMS observables (O_3, H_2O, HNO_3, NO_2, temperature) and assumed distributions of CH_4, CO, H_2, and H_2O, the exact nature of which we will show to be of minor importance. Where SAMS CH_4 data are available [*Rodgers et al.*, 1984; *Jones and Pyle*, 1984; *Jones*, 1984], they will be used. In this work we will neglect chlorine-containing compounds due to the lack of global data about them and the fact that at their current concentration ($[Cl_x] = [HCl] + [ClO] + [Cl] + [HOCl] + [ClONO_2]$) of approximately 2–3 ppbv in the stratosphere [*Berg et al.*, 1980] they are not expected to have a major effect on the concentration of HO_x species. This amount is substantially smaller than the 15–25 ppbv of NO_x expected [*Naudet et al.*, 1984; *Callis et al.*, 1985]. This model assumes all unobserved trace species to be in photochemical equilibrium, an assumption which we will test and show to be reasonable through most of the upper stratosphere for all species and through most of the stratosphere for the key reactive species O, $O(^1D)$, and NO.

Having derived an algebraic model for these concentrations $[M_i]$, we can take partial derivatives with respect to input parameters P_j (observed or assumed concentrations, rate coefficients, photolysis rates) to obtain logarithmic (dimensionless) sensitivity coefficients

$$S_{ij} = \partial(\ln [M_i])/\partial(\ln P_j) = (P_j/[M_i])(\partial[M_i]/\partial P_j) \quad (1)$$

Such sensitivity coefficients have been used widely in chemical kinetics [*Rabitz et al.*, 1983, and references therein] and have also been used in the study of atmospheric chemistry [*Butler*, 1978, 1979; *Stolarski*, 1980; P. Connell et al., private communication, 1984].

These sensitivity coefficients may be combined with the uncertainties f_j in the corresponding input parameters P_j to yield an expression for the total uncertainty u_i in calculated concentration $[M_i]$ [*Butler*, 1978, 1979; *Stolarski*, 1980; *Harries*, 1982]:

$$u_i = \exp\left[\sum_j (S_{ij} \ln f_j)^2\right]^{1/2} \quad (2)$$

The uncertainty calculated is a multiplicative factor; in other words, $[M_i]$ is uncertain in the range $[M_i]/u_i$ to $u_i[M_i]$.

The sensitivity coefficients are useful not only for their role in calculating the total uncertainty but also because of their role in providing a clear indication of which regions of the atmosphere the concentration of inferred species are sensitive to the various model input parameters. Analysis of the occurrences of large sensitivity coefficients may help pinpoint for which model input parameter(s) reduction of uncertainty would most reduce the uncertainty in the concentration of inferred species. This could be useful in assessing the need for future laboratory reaction rate and cross-section measurements as well as of in situ constituent measurements.

We have calculated sensitivity coefficients and total uncertainties for a variety of species using zonally averaged LIMS data. We will focus our attention on the reactive HO_x species OH and HO_2, deferring consideration of other species to future work.

This work is very similar in spirit to that of Pyle and coworkers [*Pyle et al.*, 1984; *Pyle and Zavody*, 1985] in which they inferred concentrations of OH, HO_2, and H_2O_2 from LIMS and SAMS data, as well as uncertainties in the inferred OH. Our approach and theirs are complementary in that they calculate uncertainties numerically by varying model input parameters within their stated uncertainties, while we calculate them analytically from partial derivatives of our algebriac model.

We should note that the development of simple algebraic models to represent upper atmospheric chemistry is not a new idea. *Leovy* [1969] developed an analytic model for photochemistry in an ozone-water vapor atmosphere and applied it to the stratosphere and lower mesosphere. *Park and London* [1974] presented a simple reaction scheme allowing the calculation of concentrations of the radical species O, H, OH, and HO_2 throughout the mesosphere and lower thermosphere. Analytic expressions relating the concentrations of these species to those of O_3 and H_2O in the mesosphere have also been presented by *Allen et al.* [1984]. Similarly, relatively simple expressions governing the total amount and partitioning of odd hydrogen ($H + OH + HO_2$) have been presented by *Brasseur and Solomon* [1984].

The outline of this paper is as follows. In section 2 the model input data and their processing are discussed, and in section 3 the algebraic model used is presented. In section 4, results are presented, primarily in the form of figures, and in section 5 they are discussed. Where available, results will be compared to those of other investigators. Finally, in section 6 a summary is presented and conclusions are offered.

2. Model Input Data and Processing

The LIMS data used were obtained from the LIMS profile tapes from the National Space Sciences Data Center (NSSDC) at the Goddard Space Flight Center. Daytime O_3, H_2O, HNO_3, NO_2, and temperature were zonally averaged and binned according to the two-dimensional grid used by *Guthrie et al.* [1984*a*] in their diabatic circulation model. Conversion of tape data to concentrations was accomplished by programs used previously [*Jackman et al.*, 1985]. In this work we will use data from the time period March 26, 1979, to April 1, 1979, corresponding roughly but not precisely to the spring equinox. This is one of the same time periods used by *Jackman et al.* [1985] in their study of LIMS HNO_3.

Rate coefficients and absorption cross sections for the model were taken from the sixth Jet Propulsion Laboratory (JPL) evaluation [*DeMore et al.*, 1983]. Photolysis rates were calculated for local noon from the model input by use of the radiation package from the two-dimensional model of *Guthrie et al.*, [1984*a*]. The assumption of local noon in the photolysis rate calculations should lead to very small errors except near 65°S, where the local time of the daytime LIMS observations was closer to 1700 LT [*Gille and Russell*, 1984].

This assumption is equivalent to one in which all the model input concentrations, especially the LIMS observables, are taken to have time-independent concentrations during daytime. This is an excellent assumption for all input species except NO_2, which has larger daytime variations [*Ko and Sze*, 1984]. Even so, its time variation is quite weak within several hours of noon. Quantification of the error introduced by this assumption would require a two-dimensional time-dependent model calculation, which has not yet been performed. Based on one set of figures from *Ko and Sze* [1984] (for 19°N in December), we estimate the possible error in using LIMS observed NO_2 concentrations as NO_2 values at noon to be almost 10–20% and then only so at high latitudes, where the local time of the LIMS observation deviates most from local noon.

Concentrations of CO, H_2, and N_2O used as model input were those obtained by *Guthrie et al.* [1984*a*, *b*] with their

TABLE 1. Uncertainty in Observed Species

Level	P, mbar	O_3	H_2O	HNO_3	NO_2	CH_4
24	1.27	15	26	NA	29	18
23	1.68	16	26	NA	24	18
22	2.24	16	24	NA	20	17
21	2.98	17	23	NA	19	17
20	3.96	18	24	NA	20	17
19	5.26	20	23	44	21	17
18	6.98	22	21	35	22	18
17	9.28	24	20	32	25	27
16	12.3	27	21	30	31	36
15	16.4	30	21	31	38	45
14	21.8	33	22	32	45	(50)
13	29.0	35	21	35	57	(47)
12	38.5	37	33	39	75	(43)
11	51.1	38	37	41	(84)	(38)
10	68.0	39	38	(41)	(84)	(35)
9	90.3	(40)	(38)	(41)	(84)	(32)
8	120.	(40)	(38)	(41)	(84)	(30)

Uncertainties are in percent. Numbers in parentheses for LIMS observables were taken by assuming constant uncertainty below the lower limits given in the various LIMS papers: O_3 [*Remsberg et al.*, 1984], H_2O [*Russell et al.*, 1984*a*], HNO_3 [*Gille et al.*, 1984*a*], and NO_2 [*Russell et al.*, 1984*b*]. For CH_4, uncertainties below level 15 were assumed as described in section 2. Pressures given are those at top of level. NA, not applicable (not used in trace species estimation).

two-dimensional model and are believed to be representative of actual stratospheric distributions. Zonally and monthly averaged SAMS CH_4 data from 20 to 0.3 mbar have been published in pictorial form [*Jones and Pyle*, 1984], and these have been visually converted into concentrations for use in our CH_4 profiles. Below 20 mbar, the profile from the *Guthrie et al.* [1984*b*] two-dimensional model was used. We will demonstrate that the exact nature of these distributions are of little significance in their effect on O_x, HO_x, and NO_x chemistry above the lower stratosphere. In the lower stratosphere their effects are significant only to total HO_x.

Uncertainties in the input concentrations for O_3, H_2O, HNO_3, and NO_2 were taken from the various LIMS validation papers: O_3 [*Remsberg et al.*, 1984], H_2O [*Russell et al.*, 1984*a*], HNO_3 [*Gille et al.*, 1984*a*], and NO_2 [*Russell et al.*, 1984*b*]. Systematic uncertainties were used, since the random contributions to the total uncertainties were essentially negligible for the LIMS species over most of the stratosphere. We neglect the uncertainty in the temperature [*Gille et al.*, 1984*b*] as this is usually considerably smaller percentage-wise than the other uncertainties, although we recognize that the strong temperature dependence of several reaction rates may make for large sensitivity coefficients with respect to temperature. Uncertainties (in percent) used for the LIMS observables are shown as a function of pressure in Table 1. Uniform uncertainties of 30% have been assumed everywhere for CO, H_2, and N_2O. For CH_4, the published uncertainties [*Jones and Pyle*, 1984] were used with the SAMS data, while a 30% uncertainty is assumed below 100 mbar. Between 20 and 100 mbar a linear interpolation of uncertainty with height was used. These are also included in Table 1.

The 30% value used for the uncertainties in the model profiles is somewhat arbitrary, but we will show that for the quantities of interest ([OH], [HO_2]) the contribution of the uncertainty of these assumed species to the total uncertainty is sufficiently small that it does not strongly affect our conclusions.

In the course of the calculations reported here, we do not use the LIMS HNO_3 values above model level 19 (approximately 5 mbar), as these have been shown to be quite high [*Gille et al.*, 1984*a*; *Jackman et al.*, 1985]. Instead, we use a version of the method developed by the latter authors to obtain upper stratospheric HNO_3 from the other LIMS observations.

Uncertainties (one standard deviation) in rate coefficients were taken from JPL evaluation 6 [*DeMore et al.*, 1983] where available. In other cases, they were estimated, although these estimated uncertainties will prove to be unimportant for the subset of the results being considered here. For uncertainties in photolysis rates we also use those listed in the JPL evaluation 6 [*DeMore et al.*, 1983]. We therefore neglect feedback effects due to variations induced in the column density of a given species above or below a given level due to changes in model input parameters. We also neglect any uncertainty in the assumed solar flux. Uncertainties in absorption coefficients are given in Table 2.

The form of reaction rate uncertainties for bimolecular reactions is that given in JPL evaluation 6 [*DeMore et al.*, 1983]:

$$f_T = f_{298} \exp\left[(\Delta E_a/R)|1/T - 1/298|\right] \tag{3}$$

Uncertainty values for the bimolecular reactions used are given in Table 3. For termolecular reactions we use analogous expressions for the low (f_0) and high (f_i) pressure limiting forms:

$$f_0 = f_{300}{}^0(300/T)^{\Delta n} \qquad T < 300 \text{ K} \tag{4a}$$

$$f_0 = f_{300}{}^0(T/300)^{\Delta n} \qquad T > 300 \text{ K} \tag{4b}$$

$$f_i = f_{300}{}^i(300/T)^{\Delta m} \qquad T < 300 \text{ K} \tag{5a}$$

$$f_i = f_{300}{}^i(T/300)^{\Delta m} \qquad T > 300 \text{ K} \tag{5b}$$

In the stratosphere where $T < 300$ K, only the former expressions will be used. Values of the parameters $f_{300}{}^0$, $f_{300}{}^i$, Δn, and Δm used are given in Table 4.

For those termolecular reactions with pressure-dependent rates the pressure-dependent uncertainties are calculated from those of the high- and low-pressure limiting reactions by use of a form of equation (2):

$$u(M, T) = \exp\{[\partial \ln k(M, T)/\partial \ln k_0(T)]^2(\ln f_0)^2 + [\partial \ln k(M, T)/\partial \ln k_i(T)]^2(\ln f_i)^2\}^{1/2} \tag{6}$$

The sensitivity coefficients in equation (6) may be evaluated analytically from the definition of $k(M, T)$, a pseudo-

TABLE 2. Photolytic Processes and Their Uncertainties

Process Number	Process	Uncertainty
1	$O_2 + h\nu \rightarrow 2O$	1.4
2	$O_3 + h\nu \rightarrow O + O_2$	1.15
3	$NO_2 + h\nu \rightarrow NO + O$	1.25
4	$O_3 + h\nu \rightarrow O(^1D) + O_2(^1\Delta)$	1.4
5[a]	$NO + h\nu \rightarrow N + O$	1.2
6	$HNO_3 + h\nu \rightarrow OH + NO_2$	1.25
7	$NO_3 + h\nu \rightarrow NO_2 + O$	2.0
8	$NO_3 + h\nu \rightarrow NO + O_2$	2.0
9	$H_2O_2 + h\nu \rightarrow 2OH$	1.4
10	$N_2O_5 + h\nu \rightarrow NO_2 + NO_3$	2.0
11	$CH_2O + h\nu \rightarrow H_2 + CO$	1.4
12	$CH_2O + h\nu \rightarrow HCO + H$	1.4
13	$H_2O + h\nu \rightarrow OH + H$	1.3
14	$N_2O + h\nu \rightarrow N + NO$	1.2
15	$HO_2NO_2 + h\nu \rightarrow HO_2 + NO_2$	2.0
16	$HO_2NO_2 + h\nu \rightarrow OH + NO_3$	2.0

[a]Uncertainty estimated.

TABLE 3. Bimolecular Reactions, Rates, and Uncertainties

Reaction No.	Process	A,[a] cm^3 molecule^{-1} s^{-1}	E_a/R, °K	f_{298}	$\Delta(E_a/R)$, °K
(R1)	$O(^1D) + N_2 \rightarrow O + N_2$	1.8(−11)	−107	1.20	100
(R2)	$O + NO_2 \rightarrow NO + O_2$	9.3(−12)	0	1.10	150
(R3)	$NO + O_3 \rightarrow NO_2 + O_2$	1.8(−12)	1370	1.20	200
(R4)	$N + O_2 \rightarrow NO + O$	4.4(−12)	3220	1.25	340
(R5)	$N + NO \rightarrow N_2 + O$	3.4(−11)	0	1.30	100
(R6)	$O(^1D) + H_2O \rightarrow 2OH$	2.2(−10)	0	1.20	100
(R7)	$O(^1D) + CH_4 \rightarrow OH + CH_3$	1.4(−10)	0	1.20	100
(R8)	$OH + O_3 \rightarrow HO_2 + O_2$	1.6(−12)	940	1.30	300
(R9)	$O + OH \rightarrow O_2 + H$	2.2(−11)	−117	1.20	100
(R10)[b]	$HO_2 + O_3 \rightarrow OH + 2O_2$	1.4(−14)	580	1.50	500
(R11)	$O + HO_2 \rightarrow OH + O_2$	3.0(−11)	−200	1.40	200
(R12)	$H + O_3 \rightarrow OH + O_2$	1.4(−10)	470	1.25	200
(R13)	$2HO_2 \rightarrow H_2O_2 + O_2$	2.3(−13)	−590	1.30	200
(R14)	$OH + HO_2 \rightarrow H_2O + O_2$	7.0(−11)	0	1.60	500
(R15)	$OH + HNO_3 \rightarrow H_2O + NO_3$	9.4(−15)	−778	1.30	100
(R16)	$NO_2 + O_3 \rightarrow NO_3 + O_2$	1.2(−13)	2450	1.15	140
(R17)	$NO + NO_3 \rightarrow 2NO_2$	2.0(−11)	0	3.00	0
(R18)[c,d]	$N_2O_5 + H_2O \rightarrow 2HNO_3$	1.0(−20)	0	1.50	200
(R19)[d,e]	$O + N_2O_5 \rightarrow 2NO_2 + O_2$	3.0(−16)	0	1.30	200
(R20)	$O(^1D) + H_2 \rightarrow OH + H$	1.0(−10)	0	1.20	100
(R21)	$OH + H_2 \rightarrow H_2O + H$	6.1(−12)	2030	1.20	400
(R22)[c,d]	$O + CH_4 \rightarrow OH + CH_3$	3.5(−11)	4550	1.20	250
(R23)	$O(^1D) + CH_4 \rightarrow CH_2O + H_2$	1.4(−11)	0	1.20	100
(R24)	$OH + CH_4 \rightarrow CH_3 + H_2O$	2.4(−12)	1710	1.20	200
(R25)	$O + CH_2O \rightarrow OH + CHO$	3.0(−11)	1550	1.25	250
(R26)	$O + CH_3 \rightarrow CH_2O + H$	1.1(−10)	0	1.30	250
(R27)	$CHO + O_2 \rightarrow HO_2 + CO$	3.5(−12)	−140	1.30	140
(R28)	$HO_2 + NO \rightarrow OH + NO_2$	3.7(−12)	−240	1.20	80
(R29)	$OH + H_2O_2 \rightarrow H_2O + HO_2$	3.1(−12)	187	1.30	200
(R30)[d]	$OH + CO \rightarrow CO_2 + H$	1.5(−13)	0	1.40	100
(R31)	$OH + CH_2O \rightarrow CHO + H_2O$	1.0(−11)	0	1.25	200
(R32)	$CH_3O_2 + NO \rightarrow CH_3O + NO_2$	3.4(−12)	−180	1.20	180
(R33)	$CH_3O + O_2 \rightarrow CH_2O + HO_2$	1.2(−13)	1350	10.0	500
(R34)	$2OH \rightarrow H_2O + O$	4.2(−12)	242	1.40	242
(R35)[d]	$CH_3 + O_2 \rightarrow CH_2O + OH$	3.0(−16)	0	1.50	200
(R36)[d,f]	$CH_3O_2 + NO \rightarrow HNO_2 + CH_2O$	8.4(−13)	−180	1.50	200
(R37)[g]	$O_2(^1\Delta) + O_2 \rightarrow 2O_2$	1.3(−18)	−163	1.20	100
(R38)	$O(^1D) + O_2 \rightarrow O + O_2$	3.2(−11)	−67	1.20	100
(R39)	$OH + HO_2NO_2 \rightarrow H_2O + NO_2 + O_2$	1.3(−12)	−380	1.50	580
(R40)	$O + NO_3 \rightarrow NO_2 + O_2$	1.0(−11)	0	1.50	150

[a] Read 1.8(−11) as 1.8×10^{-11}.
[b] Asymmetric uncertainties reported [*DeMore et al.*, 1983]; larger one used.
[c] *Hampson and Garvin* [1978].
[d] Uncertainties estimated.
[e] Upper limit.
[f] Branching ratio of 20% assumed for this channel as upper limit [*DeMore et al.*, 1983].
[g] *Hampson* [1980].

bimolecular rate constant with units of cm^3 molecule^{-1} s^{-1} [*DeMore et al.*, 1983]:

$$k(M, T) = [k_0(T)[M]/(1 + a)]0.6^{[1 + (\log_{10} a)^2]^{-1}} \quad (7)$$

where

$$a = k_0(T)[M]/k_i(T) \quad (8)$$

and the limiting rate coefficients have the form

$$k_0(T) = k_0^{300}(300/T)^n \quad (9)$$

$$k_i(T) = k_i^{300}(300/T)^m \quad (10)$$

After some straightforward algebra, the following expression for the sensitivity coefficients may be determined:

$$S_0 = \partial \ln k(M, T)/\partial \ln k_0 = 1/(1 + a) + 0.1927h^2 \ln a \quad (11a)$$

$$S_i = \partial \ln k(M, T)/\partial \ln k_i = a/(1 + a) - 0.1927h^2 \ln a \quad (11b)$$

where

$$h = [1 + 0.1886(\ln a)^2]^{-1} \quad (11c)$$

In the limit of low pressure we see that $S_0 = 1$ and $S_i = 0$, while at high pressure, $S_0 = 0$ and $S_i = 1$.

Sensitivity coefficients and total uncertainties for two of the more important pressure-dependent three-body recombination reactions

Process t_4

$$OH + NO_2 + M \rightarrow HNO_3 + M$$

Process t_8

$$HO_2 + NO_2 + M \rightarrow HO_2NO_2 + M$$

used in the model are plotted in Figure 1. We see that the total recombination rate uncertainties are largest near the tropopause where the temperature is lowest. We also see that in the upper stratosphere ($z > 35$ km), $S_0 > 0.9$, meaning that these recombination reactions should be occurring with a rate close to their corresponding low-pressure limits.

TABLE 4. Thermolecular Reactions, Rates, and Uncertainties

Reaction No.	Reaction	Low-Pressure Limiting Data				High-Pressure Limiting Data			
		k_0^{300a}	n	$f_{300}{}^0$	Δn	k_1^{300a}	m	$f_{300}{}^i$	Δm
1[b]	$O + O_2 + N_2 \rightarrow O_3 + N_2$	6.0(−34)	2.3	1.08	0.5				
2	$O + NO + M \rightarrow NO_2 + M$	1.2(−31)	1.8	1.25	0.5	3.0(−11)	0.0	1.33	1.0
3	$H + O_2 + M \rightarrow HO_2 + M$	5.5(−32)	1.6	1.09	0.5				
4	$OH + NO_2 + M \rightarrow HNO_3 + M$	2.6(−30)	3.2	1.12	0.7	2.4(−12)	1.3	1.50	1.3
5	$NO_2 + NO_3 + M \rightarrow N_2O_5 + M$	2.2(−30)	2.8	1.44	1.4	1.0(−12)	0.0	1.80	1.0
6[c]	$M + N_2O_5 \rightarrow NO_2 + NO_3 + M$	...	...	...	...	...	...	...	...
7	$CH_3 + O_2 + M \rightarrow CH_3O_2 + M$	6.0(−31)	2.0	1.50	1.0	2.0(−12)	1.7	1.50	1.7
8	$HO_2 + NO_2 + M \rightarrow HO_2NO_2 + M$	2.3(−31)	4.6	1.09	1.0	4.2(−12)	0.0	1.24	2.0
9	$O + NO_2 + M \rightarrow NO_3 + M$	9.0(−32)	2.0	1.11	1.0	2.2(−11)	0.0	1.14	1.0
10[d]	$2OH + M \rightarrow H_2O_2 + M$	6.9(−31)	0.8	1.43	2.0	1.0(−11)	1.0	1.50	1.0
11[e]	$2HO_2 + M \rightarrow H_2O_2 + M$	...	...	...	...				
12	$O + 2O_2 \rightarrow O_3 + O_2$	6.4(−34)	2.3	1.08	0.5				
13[f]	$OH + CO + M \rightarrow CO_2 + H$	...	...	1.40	0.0				

[a]Read 6.0(−34) as 6.0×10^{-34}. For low-pressure limit; k is in units of cm^6 molecule^{-2} s^{-1}; for high-pressure limit, k is in units of cm^3 molecule^{-1} s^{-1}.
[b]Ratio t_{12}/t_1 is that given by NASA [1979].
[c]$t_6 = t_5/K_{eq}$, $K_{eq} = 1.77(-27) \exp(11001/T)$, $f_{300} = 1.5$, $\Delta(E/R) = 500$ (assumed).
[d]Asymmetrical error limits [*DeMore et al.*, 1983]; larger of two used here.
[e]$t_{11} = 1.7(-33) \exp(1000/T)$ [M].
[f]$t_{13} = 9(-14)P_{atm}$.

3. Algebraic Model Used

The algebraic model we have developed should be applicable for daylight conditions (recall that most daytime LIMS observations were made at times close to local noon). It assumes that all molecules other than those observed are in photochemical equilibrium or obtained from two-dimensional model calculations. Since the input species control O_x, HO_x, NO_x, and hydrocarbon oxidation chemistry, we may calculate concentrations and uncertainties for the following set of species: O, $O(^1D)$, NO, OH, H, HO_2, H_2O_2, CH_2O, HO_2NO_2, CH_3, CH_3O_2, CH_3O, CHO, $O_2(^1\Delta)$, N_2O_5, NO_3, and N. We will focus our attention on OH and HO_2, deferring studies of other species to future publications. As mentioned earlier, we do not include chemistry of Cl-containing species, although we do consider the effect of their neglect on our results.

In attempting to set up an algebraic model for stratospheric O_x, NO_x, and HO_x chemistry in a LIMS-constrained stratosphere, one must establish a balance between the goals of accuracy and simplicity of expressions. The complex nature of stratospheric chemistry makes the development of an exact analytic model impossible. In order to obtain sufficiently simple expressions suitable to extensive differentiation, we must make approximations, retaining only the chemically most significant terms. In doing so, the accuracy of the expressions is of necessity going to be sacrificed. We examine in some detail the accuracy of the expressions used in our model in Appendix B.

The advantage of having an algebraic (or mostly algebraic) model is the ability to see relatively simply the effects of variation of model input parameters as well as to help one gain a better intuitive feeling for the processes operating in stratospheric chemistry. If one is solely interested in inferring trace species concentrations without being concerned about sensitivities and uncertainties, there is really no great advantage to using an algebraic model, as fast numerical methods are available for solving the coupled steady state equations.

The set of photolysis processes (Table 2) and chemical reactions (Tables 3 and 4) included in the model has been determined by detailed analysis of production and loss terms in a series of runs of a one-dimensional atmospheric photochemical model [*Herman*, 1979] with a single fixed ozone profile for a variety of solar zenith angles. Since this model has a very large data base of chemical reactions, only the most important ones for the species listed above have been retained

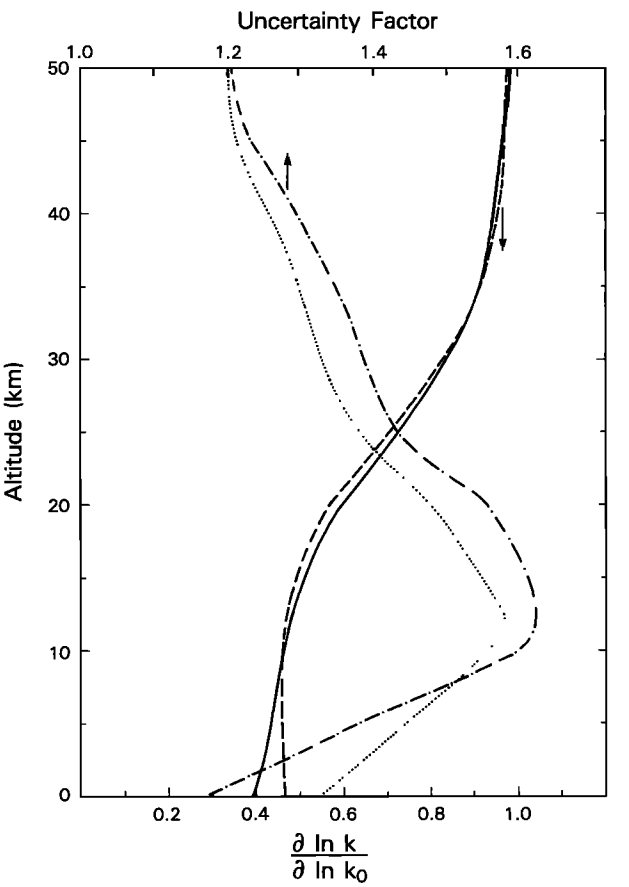

Fig. 1. Sensitivity coefficients (total recombination rate to low-pressure limiting rate) and total uncertainties for selected pressure-dependent tertiary recombination reactions as a function of height for U.S. Standard Atmosphere (1976) for processes t_4 and t_8. Curves with downward pointing arrows are for sensitivity coefficients and refer to lower abscissa (t_4, solid line; t_8, dashed line); curves with upward pointing arrows are for total uncertainties, and refer to upper abscissa (t_4, dotted line; t_8, dashed-dotted line).

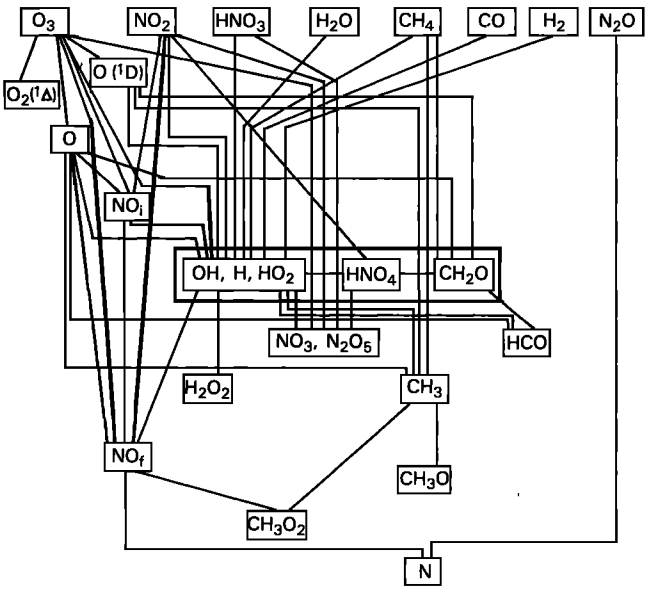

Fig. 2. Schematic diagram indicating hierarchy of expressions used to calculate trace species concentrations. LIMS observables and assumed species are on the top row. Lines connect species whose concentrations contribute to the calculation of other species to those other species. Lines are assumed to point downward (species at upper end of line affect those at lower end). Boxed species are calculated simultaneously by iteration.

for this work. Agreement between the one-dimensional model results and those of the approximate algebraic model was almost always to within 10% and usually much better than that (especially in the upper stratosphere where the chemistry is simpler), and this was deemed to be more than adequate.

Where possible, we derived analytic expressions for the concentrations of the unobserved trace species, but an iterative scheme was necessary to determine most of the desired concentrations. The iteration scheme usually converged to within 0.1% after fewer than 10 iterations. The nature of the "hierarchy" of approximations made in deriving the algebraic model may be seen in Figure 2, in which lines are drawn to

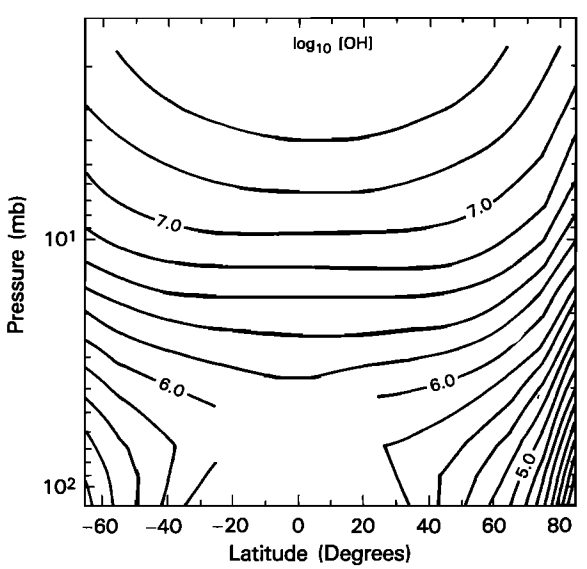

Fig. 3. Two-dimensional (pressure versus latitude) contour plot of base 10 logarithm of OH concentration calculated using HO_x sources and sinks method (method A). Contours are spaced every 0.2 log units. The blank area in the tropical lower stratosphere corresponds to areas where complete LIMS data are not available.

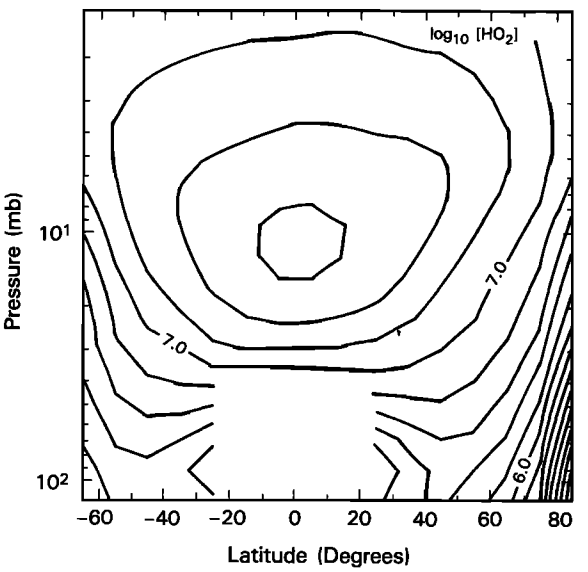

Fig. 4. Two-dimensional contour plot of base 10 logarithm of HO_2 concentration calculated by method A. Labeling is as in Figure 3.

indicate which calculated species depend on the concentrations of observed, assumed, or other calculated species. Lines can be thought of as pointing down: the species at the upper end of the lines are used in obtaining the concentration of the species at the lower end of the line. The box enclosing OH, H, HO_2, HO_2NO_2, and CH_2O indicates that these species are allowed to vary simultaneously and are thus determined by iteration. NO_3 and N_2O_5 are included in another box to indicate that they are solved for simultaneously. A single iteration is performed for NO; the initial estimate is labeled NO_i and the final estimate is labeled NO_f. Equations used in the algebraic scheme are shown in Appendix A.

Derivation of the formulas for O, $O(^1D)$, $O_2(^1\Delta)$, and NO (initial estimate) are straightforward from the assumed reaction set (Tables 2–4), and we do not elaborate on these. The validity of these and all other expressions is examined in Appendix B.

The equation for OH, the key constituent on which most other derived constituents depend (see Figure 2), is more complicated, and we briefly outline its derivation here. We start by assuming that the total odd hydrogen concentration [*Rundel et al.*, 1978] $[HO_x] = [OH] + [H] + [HO_2] + [HNO_3] + [HO_2NO_2] + 2[H_2O_2] + [CH_3] + [CH_3O] + [CH_3O_2] + [HCO]$ is in photochemical equilibrium (equal production P and loss L rates)·

$$P(HO_x) = L(HO_x) \tag{12}$$

where, neglecting certain small terms (i.e., k_{18}, k_{22})

$$x = P(HO_x) = 2\{(J_{13} + k_6[O(^1D)])[H_2O] + k_7[O(^1D)][CH_4] + k_{20}[O(^1D)][H_2] + (J_{12} + k_{25}[O])[CH_2O]\} \tag{13a}$$

$$L(HO_x) = 2[OH](k_{14}[HO_2] + k_{15}[HNO_3] + k_{39}[HO_2NO_2] + k_{34}[OH]) \tag{13b}$$

In attempting to solve equation (12) via equation (13), we see that $[HO_2]$, $[HO_2NO_2]$, and $[CH_2O]$ must also be determined (as must $[HNO_3]$ in regions where LIMS HNO_3 is unreliable). The equations relating these species to [OH] are given in Appendix A. Combining equations (12), (13), and (A9)–(A13), one can show simply

$$[OH] = [-w + (w^2 + 8xv)^{1/2}]/(4v) \tag{14}$$

where

$$v = k_{14}E/D + k_{34} \quad (15)$$

$$w = 2(k_{15}[HNO_3] + k_{39}[HO_2NO_2]) \quad (16)$$

the ratio E/D is approximately the ratio of $[HO_2]$ to [OH] (see Appendix A); w is thus related to the rate of loss of HO_x by reaction of OH with NO_x, while v is related to that due to reaction with other H-containing species.

With the exception of NO_3 and N_2O_5, the derivation of all remaining expressions for the trace species concentrations is straightforward. Formulas are given in equations (A18)–(A23). NO_3 and N_2O_5 must be determined simultaneously, and this is done using the pair of equations (constants are defined in equations (A26)–(A30))

$$d[NO_3]/dt = 0 = B_1 - A_{11}[NO_3] + A_{12}[N_2O_5] \quad (17a)$$

$$d[N_2O_5]/dt = 0 = A_{21}[NO_3] - A_{22}[N_2O_5] \quad (17b)$$

Since N_2O_5 is known to have a slow time dependence which is a strong function of altitude during the day [*Fabian et al.*, 1982], these expressions are not expected to yield accurate values of $[N_2O_5]$ over the whole stratosphere. Regions of validity are discussed in Appendix B.

At altitudes above the 5-mbar pressure level where the LIMS HNO_3 values as currently analyzed appear to be unphysically high [*Jackman et al.*, 1985], the HNO_3 values are not used, and $[HNO_3]$ is instead determined by assuming it to be in photochemical equilibrium. In that case an alternative expression for [OH] (in which HNO_3 is included in the iteration), presented in the Appendix A, is needed.

Sensitivity coefficients are taken by analytically evaluating partial derivatives with respect to input concentrations, rate coefficients, and photolysis rates. Iterations are performed for the sensitivity coefficients of OH, H, HO_2, HO_2NO_2, and CH_2O (and HNO_3 where the LIMS values are not used).

The method here for inferring the concentration of odd hydrogen species is substantially different from the method used by *Pyle et al.* [1983, 1984], in which OH is inferred from the LIMS observations of NO_2 and HNO_3 by the assumption of photochemical equilibrium of HNO_3. This assumption leads to a very simple expression for OH:

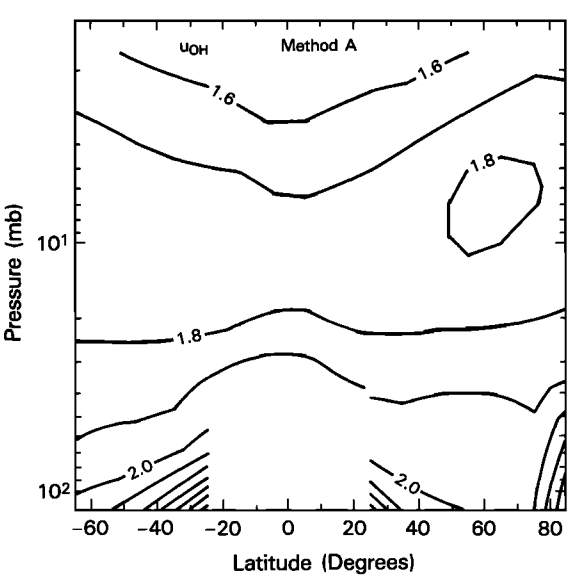

Fig. 5. Two-dimensional plot of uncertainty factors for OH calculated using the sources and sinks method. The contour spacing is 0.1.

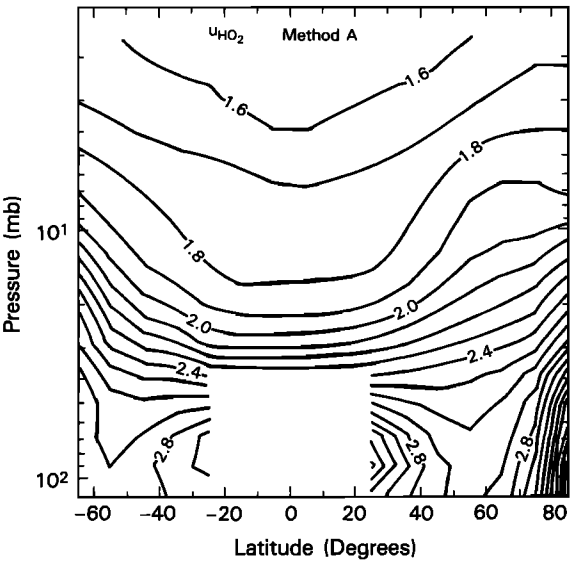

Fig. 6. Two-dimensional plot of uncertainty factors for HO_2. Contour spacing is 0.1.

$$[OH] = \frac{J_6[HNO_3]}{t_4[NO_2] - k_{15}[HNO_3]}$$

4. Results

The results of this study consist of concentrations, sensitivity coefficients, and total uncertainties for the trace species enumerated earlier as a function of latitude and altitude. This is a vast amount of information, and we consider here only a small subset of these results. In particular, we will consider latitude and altitude variation of OH and HO_2 concentrations and their total uncertainties. In this section we will point out some of the key features of the quantities shown; comments on their origin, significance, and relationship to work of others will be deferred to the ensuing discussion section.

Concentrations, either in the form of base 10 logarithms of number densities for OH and HO_2 as a function of latitude and altitude are given in Figures 3 and 4, respectively. OH concentrations (Figure 3) are relatively insensitive to latitude, except near the poles, where they decrease as one moves poleward; this decrease becomes more prominent as one goes to higher altitudes. Lowest OH values are found in the polar lower stratosphere. [OH] is seen to increase with altitude nearly everywhere in the stratosphere. HO_2 (Figure 4) has a substantially different distribution, having a strong maximum in the tropical midstratosphere (near 10 mbar) and much larger latitudinal dependence in the upper and lower stratosphere than does OH. Through the midstratosphere and lower stratosphere, $[HO_2] > [OH]$ nearly everywhere; $[OH] > [HO_2]$ only above approximately 4 mbar.

Total uncertainties of OH and HO_2 as a function of latitude and altitude are shown in Figures 5 and 6, respectively. We see that u_{OH} and u_{HO_2} are of the same magnitude throughout most of the stratosphere and that the total uncertainties have only mild latitude dependence except in the very lower part of the stratosphere, especially the tropics (both species) and north polar region (HO_2). For ease of comparison, total uncertainties for the calculated HO_x species OH and HO_2 are shown for 35°N as a function of altitude of Figure 7 along with the additional HO_x species H, H_2O_2, and HO_2NO_2. Clearly, $u_{H_2O_2}$ is the greatest, followed by $u_{HO_2NO_2}$. In the lower stratosphere, $u_{HO_2} > u_{OH}$, while in the upper stratosphere they are roughly equal.

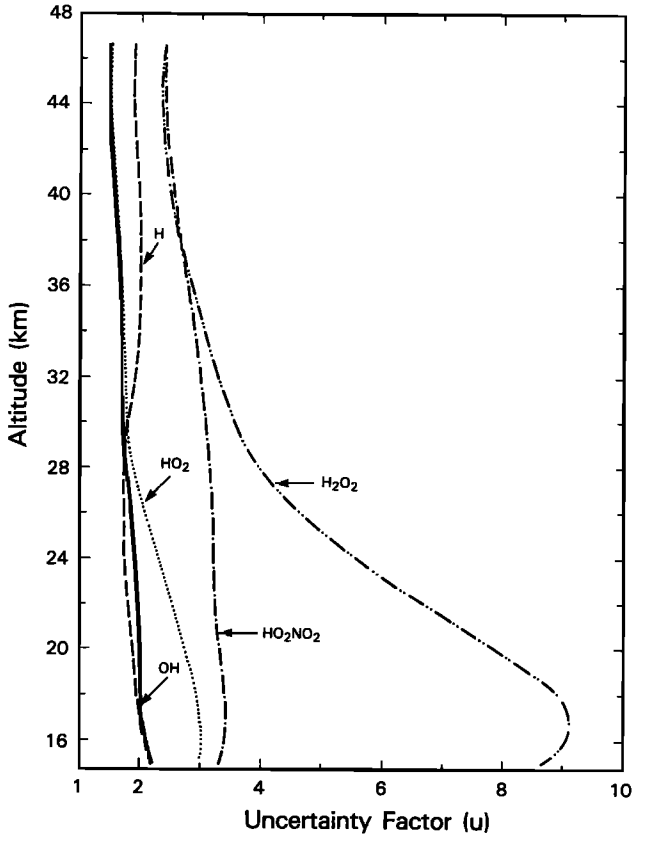

Fig. 7. Uncertainty factors of HO_x species as a function of height for 35°N.

5. Discussion

In this section we will consider separately the results presented in the previous section for concentrations of OH and HO_2 (section 5.1) and their total uncertainties (section 5.2), treating sensitivity coefficients only as necessary. A full discussion of the sensitivity coefficients obtained will be deferred to a future publication.

5.1. *Concentrations*

We will comment relatively briefly on the OH distribution calculated here because the estimation of [OH] from LIMS data has been dealt with extensively elsewhere [*Pyle et al.*, 1983, 1984; *Jackman et al.*, 1985]. The results of this model are, as expected, very similar to those of the latter authors, and their discussion of the relationship between the [OH] values obtained using their numerical sources and sinks method and the HNO_3/NO_2 method of the former authors carries over to this work. There are substantial differences between the total uncertainties derived from the two methods, however, and we will discuss this point extensively below.

There exist substantially fewer measurements of HO_2 in the stratosphere than of OH, so our ability to compare the derived HO_2 concentrations (Figure 4) to previous data is limited. *Mihelcic et al.* [1978] estimated a mixing ratio of 0.1 ppbv for HO_2 at 53°N, 31.8 km, on August 8, 1976, just after dawn (solar zenith angle 85°). This value corresponds to a number density for $[HO_2]$ of 2.9×10^7 cm^{-3}, where the conversion from mixing ratio to number density is done using the U.S. Standard Atmosphere [1976]. Due to expected diurnal variation of HO_2 (see, for example, *Fabian et al.* [1982]) at midday a somewhat higher value of HO_2 would be expected; the *World Meteorological Organization* (WMO) [1982] suggested a factor of 2 enhancement at midday.

Anderson et al. [1981] flew a balloon-borne device which converted HO_2 to OH by (R28), and then used resonance fluorescence to detect the additional OH. They obtained data at 32°N from 29 to 37 km in September, November, and December 1977 with the solar zenith angle being 41°, 45°, and 50°, respectively, and found HO_2 mixing ratios from less than 0.07 ppbv up to 0.82 ppbv. Most recently, *de Zafra et al.* [1984] measured stratospheric HO_2 by ground-based millimeter-wave spectroscopy from 4 hours after sunrise to 1 hour before sunset at 19.5°N in September and October 1982 and obtained results which suggest that they were seeing smaller HO_2 values below 35 km than were found by *Anderson et al.* [1981].

We have plotted the results of *Mihelcic et al.* [1978] and *Anderson et al.* [1981] (that of the former is multiplied by a factor of 2, as suggested by *WMO* [1982]), along with our results at 45°N in Figure 8. Since our results were obtained for times close to the equinox (where the ecliptic is at 3°N), the solar zenith angle at 45°N is close to 42°, which is very close to the mean solar zenith angle at local noon for the time and latitude of the measurements of *Anderson et al.* [1981] (ecliptic at 11°S, latitude 32°N). It is seen that those measurements are compatible with the LIMS-derived values above 35 km but are below them below 35 km, although it is not conclusive evidence. This lends support to the suggestions of *de Zafra et*

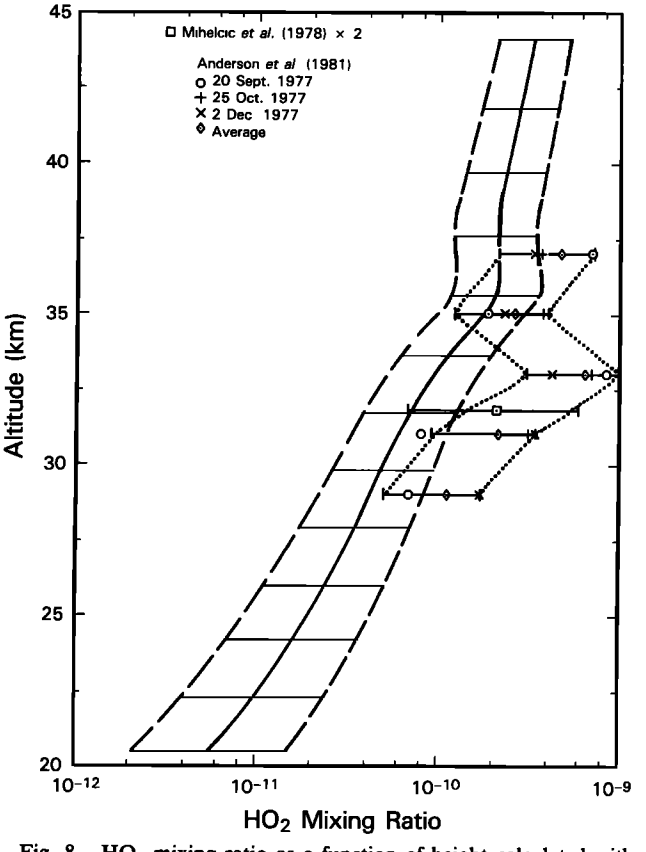

Fig. 8. HO_2 mixing ratio as a function of height calculated with HO_x sources and sinks method at 45°N. Approximately parallel curves reflect upper and lower bounds estimated by use of uncertainty factors calculated. Points and associated error bars represent experimental observations as indicated. Error bars for measurements of *Anderson et al.* [1981] are for average of three measurements. Value of *Mihelcic et al.* [1976] has been multiplied by a factor of 2, as described in the text.

TABLE 5. Sensitivities and Uncertainties of OH From Sources and Sinks (35°N)

j	$S_{[OH],j}$	f_j	$S \ln (f)$
	3 mbar (40 km)		
k_{14}	−0.482	2.12	−0.363
k_{11}	0.430	1.57	0.193
J_4	0.567	1.40	0.191
k_6	0.427	1.27	0.102
$[H_2O]$	0.473	1.23	0.098
k_8	−0.211	1.54	−0.091
k_1	−0.312	1.27	−0.075
k_9	−0.271	1.27	−0.065
$[O_3]$	0.406	1.17	0.064
	16 mbar (28 km)		
k_8	−0.517	1.78	−0.299
k_{14}	−0.239	2.71	−0.238
J_4	0.569	1.40	0.191
k_3	−0.341	1.48	−0.134
k_6	0.454	1.33	0.130
k_1	−0.383	1.33	−0.110
t_8	−0.287	1.39	−0.095
$[H_2O]$	0.488	1.21	0.093
k_{28}	0.341	1.31	0.091
J_3	0.320	1.26	0.073
	90 mbar (17 km)		
k_{39}	−0.258	3.36	−0.313
k_8	−0.364	1.97	−0.247
J_4	0.667	1.40	0.225
t_8	−0.380	1.66	−0.193
k_{15}	−0.468	1.49	−0.188
$[H_2O]$	0.505	1.38	0.163
k_6	0.503	1.38	0.162
$[HNO_3]$	−0.466	1.41	−0.160
k_3	−0.338	1.58	−0.156
k_1	−0.457	1.38	−0.147
k_{28}	0.338	1.34	0.099
$[CH_4]$	0.327	1.30	0.086
J_3	0.337	1.26	0.076

al. [1984] that the results of *Anderson et al.* [1981] may be high below 35 km, although it is not conclusive evidence. The one data point for *Mihelcic et al.* [1978] scaled as defined previously is above the LIMS-derived value, but there is appreciable overlap in the error bars. There are no published measurements for HO_2 below 29 km, so one cannot make any statement concerning the accuracy of the inferred HO_2 profile in the lower stratosphere. We emphasize that the uncertainty factors for HO_2 there are large (close to 2.5), so that comparison with any measurements that might be made should be done cautiously.

Two-dimensional model calculations [*Miller et al.*, 1981] have also obtained lower values for stratospheric HO_2 than the average of the values of *Anderson et al.*. [1981], but one should not ascribe too much importance to this, as there have been many changes in the recommended HO_x reaction rates since those calculations were completed, especially k_{11}, k_{14}, and k_{39}. The LIMS-derived values and the two-dimensional model of *Miller et al.* [1981] do agree in that both have the maximum HO_2 concentration for a given altitude near the equator (see Figure 4). *Garcia and Solomon* [1983], however, obtained fairly good agreement between the HO_2 calculated in their two-dimensional model and that measured by *Anderson et al.* [1981]. In the 30–35 km range the results for HO_2 derived here fall in the middle of their mid-latitude range [*Garcia and Solomon*, 1983, Figure 20], but below approximately 28 km, the HO_2 concentrations derived here fall below their values. This may be due to their neglect of HO_2NO_2, which through (R39) is an important HO_x sink in the lower stratosphere.

5.2. *Uncertainties*

Two important conclusions were obtained from our study of uncertainties of trace species concentrations. First, it was seen that different species can have dramatically different uncertainty factors (see Figure 7), even though all are inferred from the same data base. Further, the altitude dependence of the inferred uncertainty factors varied substantially from one species to the next. Second, the different inference schemes used for OH (HO_x sources and sinks, the HNO_3/NO_2 ratio method) can lead to substantially different uncertainty factors.

In order to understand in detail the origin of the uncertainty factors calculated, it is necessary to carefully consider the sensitivity coefficients for a given species with respect to all model input parameters. We will consider here only the sensitivity coefficients for OH and HO_2 with the largest magnitudes at three altitudes corresponding to the lower, middle, and upper stratosphere at 35°N. We then combine these with the uncertainties in the corresponding parameter to see what input parameters most contribute to the total uncertainty. This analysis is similar to that carried out by *Stolarski* [1980] in his sensitivity study of stratospheric chemistry.

Sensitivity coefficients S, parameter uncertainty factors f, and their appropriate products ($S \ln (f)$) are given for OH and HO_2 in Tables 5 and 6, respectively, where the OH has been derived from the HO_x sources and sinks method (hereafter referred to as method A). Those for OH and HO_2 derived from the HNO_3/NO_2 ratio method (hereafter referred to as method B) are given in Tables 7 and 8, respectively. For the latter method, only low and middle stratosphere values are displayed because the LIMS HNO_3 values, on which method B strongly relies, are unphysically high above approximately 5 mbar [*Jackman et al.*, 1985].

In general, uncertainty factors are considerably larger in the lower stratosphere than they are in the upper stratosphere. The magnitude of this difference varies from one species to the next. This may be seen by examination of Figures 5 and 6 or in summary in Figure 7. Clearly, OH and H have only limited height dependence in their uncertainties, while that of HO_2, HO_2NO_2, and H_2O_2 is much larger.

This height dependence derives from two sources, as may be seen in equation (2). First, the uncertainties in the model input parameters are greater in the lower stratosphere. The LIMS measurements are most uncertain in the lower stratosphere (Table 1), and the low temperatures of the lower stratosphere mean that reaction rate uncertainties, calculated as described earlier, are larger there also. Uncertainties in photolysis rates are assumed to be independent of height. Second, sensitivity coefficients in many cases become larger in magnitude in the lower stratosphere than they are in the upper stratosphere. This is particularly true for sensitivity coefficients with respect to NO_2 and HNO_3, which are quite small in the upper stratosphere, where $[HNO_3]$ and daytime $[NO_2]$ are small. Since these species have very large uncertainties in their measured amounts in the lower stratosphere, it is expected that molecules whose concentrations are sensitive to that of NO_2 and HNO_3 will thus have very large uncertainties in the lower stratosphere.

This analysis explains, for example, why the altitude variation of the OH uncertainty is much smaller than that of HO_2 (see Figures 5–7). For OH, many of the important parameters affecting its concentration have approximately equal sensitivity coefficients throughout the stratosphere, most importantly $[H_2O]$, J_4, k_6, and k_1 (see Table 5). Other parameters figure most importantly in the upper stratosphere ($[O_3]$, k_{14}, k_{11}) or

TABLE 6. Sensitivities and Uncertainties of HO_2 From Sources and Sinks (35°N)

j	$S_{[HO_2],J}$	f_j	$S \ln (f)$
	3 mbar (40 km)		
k_{14}	−0.481	2.12	−0.362
k_{11}	−0.460	1.57	−0.207
J_4	0.314	1.40	0.106
k_8	0.224	1.54	0.104
k_6	0.425	1.27	0.102
$[H_2O]$	0.474	1.23	0.098
$[O_3]$	0.485	1.17	0.076
k_1	−0.317	1.27	−0.076
k_9	0.289	1.27	0.069
	16 mbar (28 km)		
$[O_3]$	1.132	1.30	0.297
k_8	0.445	1.78	0.257
k_{14}	−0.236	2.71	−0.235
$[NO_2]$	−0.611	1.38	−0.197
J_4	0.541	1.40	0.174
k_{39}	−0.135	2.76	−0.137
k_6	0.448	1.33	0.129
k_3	0.299	1.48	0.117
k_1	−0.395	1.33	−0.114
t_8	−0.304	1.39	−0.100
$[H_2O]$	0.484	1.21	0.092
k_{28}	−0.299	1.31	−0.080
J_3	−0.287	1.25	−0.065
k_{38}	−0.150	1.33	−0.043
$[CH_4]$	0.145	1.30	0.038
	90 mbar (17 km)		
$[NO_2]$	−0.887	1.84	−0.541
$[O_3]$	1.553	1.40	0.523
k_8	0.511	1.97	0.347
k_{38}	−0.264	3.36	−0.320
k_3	0.476	1.58	0.219
J_4	0.646	1.40	0.207
t_8	−0.409	1.66	−0.207
k_{15}	−0.451	1.49	−0.181
$[H_2O]$	0.494	1.38	0.159
k_6	0.486	1.38	0.156
$[HNO_3]$	−0.455	1.41	−0.156
J_{15}	0.217	2.00	0.150
k_1	−0.465	1.38	−0.149
k_{28}	−0.476	1.34	−0.140
J_3	−0.476	1.25	−0.108
$[CH_4]$	0.372	1.30	0.098

in the lower stratosphere ($[HNO_3]$, k_{15}, t_8, k_8, k_{28}). For HO_2 a much larger number of input parameters contribute to the total uncertainties than do for OH, especially in the lower stratosphere. While those making an essentially altitude-independent contribution for OH also do so for HO_2, the altitude-dependent parameters have a much larger altitude variation than do those for OH. In particular, sensitivity coefficients of HO_2 with respect to $[O_3]$ and $[NO_2]$ are very large in magnitude in the lower stratosphere, while those of OH with respect to $[O_3]$ and $[NO_2]$ are small there. Thus one sees that a major part of the total uncertainty for HO_2 there comes from input parameters to which OH is barely sensitive at the same altitude.

TABLE 7. Sensitivities and Uncertainties of OH From HNO_3/NO_2 Ratio Method (35°N)

j	$S_{[OH],J}$	f_j	$S \ln (f)$
	16 mbar (28 km)		
$[NO_2]$	−1.158	1.38	−0.373
t_4	−1.158	1.34	−0.339
$[HNO_3]$	1.158	1.31	0.313
J_6	1.000	1.25	0.223
k_{15}	0.158	1.44	0.058
	90 mbar (17 km)		
$[NO_2]$	−1.229	1.84	−0.749
t_4	−1.229	1.57	−0.554
$[HNO_3]$	1.229	1.41	0.422
J_6	1.000	1.25	0.223
k_{15}	0.229	1.49	0.091

TABLE 8. Sensitivities and Uncertainties of HO_2 From HNO_3/NO_2 Ratio (35°N)

j	$S_{[HO_2],J}$	f_j	$S \ln (f)$
	16 mbar (28 km)		
$[NO_2]$	−1.814	1.38	−0.584
k_8	0.957	1.78	0.553
t_4	−1.152	1.34	−0.337
$[O_3]$	1.238	1.30	0.325
$[HNO_3]$	1.153	1.31	0.311
k_3	0.628	1.48	0.247
J_6	0.995	1.25	0.222
k_{10}	−0.205	2.54	−0.191
k_{28}	−0.628	1.31	−0.168
J_3	−0.604	1.25	−0.137
k_{15}	0.157	1.44	0.058
	90 mbar (17 km)		
$[NO_2]$	−2.072	1.84	−1.263
k_8	0.862	1.97	0.586
t_4	−1.206	1.57	−0.554
$[O_3]$	1.488	1.40	0.501
$[HNO_3]$	1.221	1.41	0.420
k_3	0.766	1.58	0.353
k_{28}	−0.766	1.34	−0.225
J_6	0.981	1.25	0.219
J_3	−0.765	1.25	−0.174
k_{15}	0.225	1.49	0.090

The reasons why total uncertainties for HO_2NO_2 and H_2O_2 are greater than those for OH and HO_2 can be seen by consideration of the expressions relating their concentrations (equations (A13) and (A18)). For HO_2NO_2, contributions to the total uncertainty will come from OH, HO_2, NO_2, and the processes t_8, k_{39}, J_{15}, J_{16}. With the exception of t_8, each of these latter set of parameters has uncertainty factors u_j greater than or equal to 2 throughout the stratosphere, leading to the large total uncertainty for HO_2NO_2. For H_2O_2, large total uncertainties are expected, since the quadratic dependence of $[H_2O_2]$ on $[HO_2]$ leads one to expect H_2O_2 sensitivity coefficients to be essentially twice those of HO_2, and this is indeed seen to be the case. Since the sensitivity coefficients are exponentiated in calculating the total uncertainty (equation (2)), it is expected that such doubling of S should lead to an approximate squaring of the total uncertainty. This behavior may be seen in Figure 7. The extreme sensitivity of H_2O_2 and HO_2NO_2 to model input parameters has been noted previously by *Derwent and Eggleton* [1981].

The relationship between the uncertainty factors for OH and HO_2 calculated using method A and those using method B in the upper stratosphere may be seen by comparing Figures 5 and 6 with Figures 9 and 10, which show the two-dimensional distributions of uncertainty factors from method B for OH and HO_2, respectively. For OH the higher-altitude uncertainties are approximately equivalent, but a discrepancy arises as altitude decreases as the uncertainties for method B become larger than those from method A. This low-altitude discrepancy is considerably larger for HO_2 than it is for OH.

The origin of these effects can be seen in Tables 7 and 8, in which sensitivity coefficients, uncertainty factors, and individual contributions to the total uncertainty are shown for method B. OH uncertainties are larger using method B for

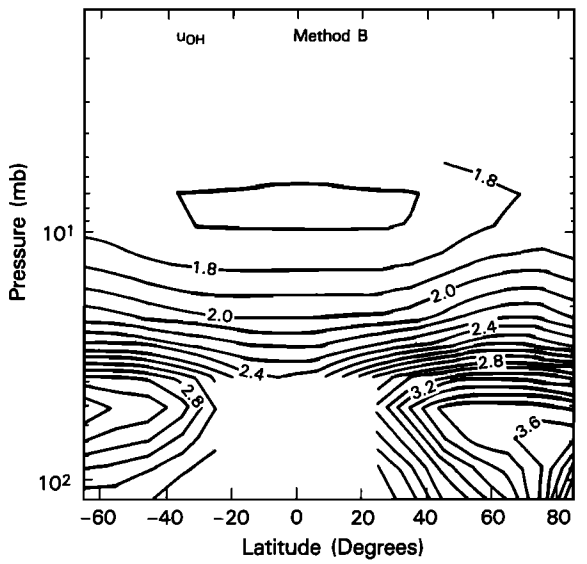

Fig. 9. Two-dimensional plot of uncertainty factors for OH calculated using the ratio method. Contour spacing is 0.1.

two reasons. First, in method B, OH is very sensitive to NO_2, HNO_3, t_4, J_6, and k_{15}, and large sensitivity coefficients lead to large total uncertainties when the corresponding parameter uncertainties are not very small. Second, some of the input parameters, notably $[NO_2]$ and $[HNO_3]$, on which method B relies are among the more uncertain. The altitude dependence for the total uncertainty in this method comes almost entirely from that of these two model input parameters; the altitude variation of the sensitivity coefficients and of the uncertainty in t_4, J_6, and k_{15} is small or nonexistent.

The uncertainty factors estimated here for OH are larger than the 40% estimated by *Pyle et al.* [1983]. This difference comes mainly from the fact that the uncertainties in the LIMS HNO_3 and NO_2 values (see Table 1) are larger than the 25% they assumed and partially from the errors in t_4 and J_6. As they noted, the $[HNO_3]/[NO_2]$ ratio might be less uncertain than one would expect by combining the uncertainties in $[HNO_3]$ and $[NO_2]$ and assuming uncorrelated errors in the

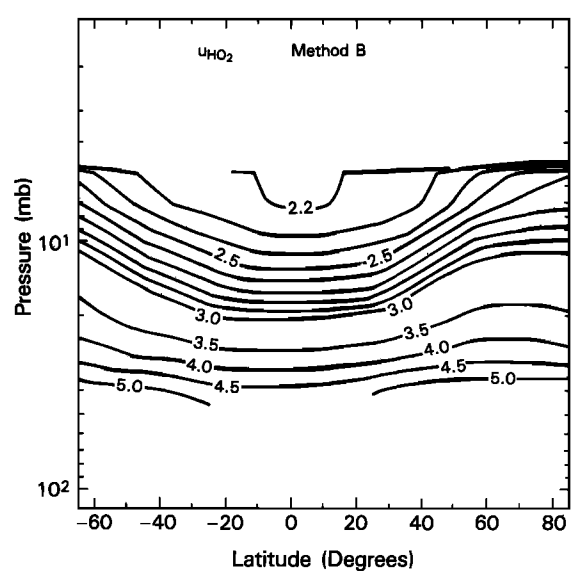

Fig. 10. Two-dimensional plot of uncertainty factors for HO_2 as in Figure 9. Contour spacing is 0.1 for contours below 3.0 and 0.5 above it.

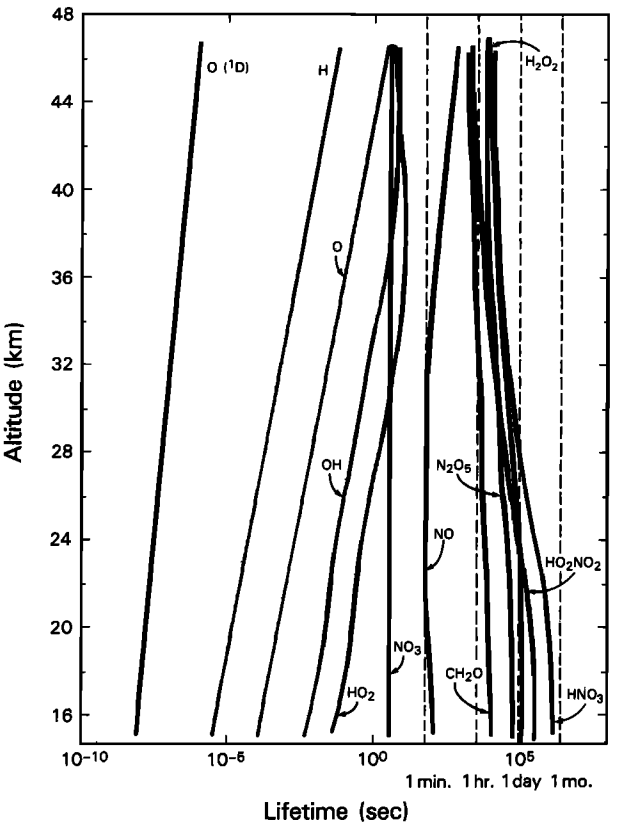

Fig. 11. Plot of lifetimes of various species as a function of altitude for 35°N, calculated using concentrations obtained with the sources and sinks method. Dashed lines indicate (from left to right) times corresponding to 1 min, 1 hour, 1 day, and 1 month.

LIMS measurements of these species, as we have done here. This reduction in uncertainty might be due to systematic errors in the inversion and/or retrieval algorithm for both HNO_3 and NO_2. Since it is this ratio that is used in the application of method B (and not individual concentrations), it is conceivable, therefore, that a reduced value for OH uncertainty for this method might be obtained.

Unlike OH, in method B, HO_2 depends sensitively (the magnitude of the sensitivity coefficient is greater than 0.5) on a number of parameters, with especially large sensitivity to NO_2, the least well determined of the LIMS observables. As may be seen in equation (2), sensitivity coefficients enter into the total uncertainty in a nonlinear way, with large sensitivities (those greater than one) contributing greatly to the sum. Thus the latter method, while being reasonably well suited to estimation of OH, leads to large uncertainties in the inferred HO_2 if equation (2) is used directly.

An alternative way to infer the uncertainty of HO_2 for method B might be to break HO_2 into its component parts

$$[HO_2] = R[OH]$$

where R is the HO_2/OH ratio, so that the uncertainty in HO_2 will now be given by the expression

$$u_{HO_2} = \exp\,[(\ln u_R)^2 + (\ln u_{OH})^2]^{1/2}$$

Such an expression would lead to reduced uncertainties for HO_2 because now the large sensitivity of HO_2 with respect to $[NO_2]$ would be broken up into two parts, and therefore two sensitivity coefficients of -1 would contribute to the total uncertainty rather than one of -2.

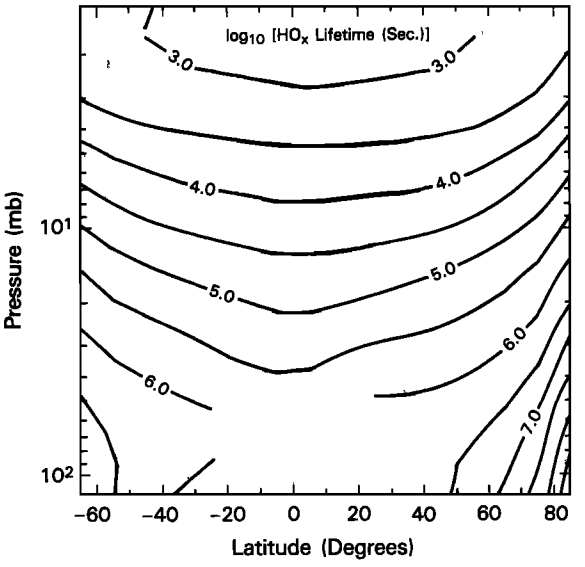

Fig. 12. Two-dimensional plot of the base 10 logarithm of HO_x lifetime (in seconds) calculated using concentrations obtained with the sources and sinks method. Contour interval is 0.5 log units.

5.3. *Validity of Photochemical Equilibrium Assumption*

The ability to easily and accurately infer trace species concentrations from the LIMS data rests on the validity of the photochemical equilibrium assumption. If one may not invoke this assumption, such inference will be much more complicated, requiring the use of diurnally varying solar fluxes and integration of the chemical rate equations or, at least, the use of an improved way of accounting for diurnal variation (i.e., the approach of *Turco and Whitten* [1978]). Photochemical equilibrium is satisfied when the lifetime of a given species or a group of species (such as HO_x) is shorter than the time scale for other processes, such as solar variation or transport.

The use of zonally averaged data makes the fast zonal transport of little consequence, and meridional transport is sufficiently slow away from the polar regions that one might need up to ten days for transport over the 10° latitude grid used here. Vertical transport is extremely slow and provides no limitation on the use of the photochemical equilibrium assumption for HO_x species given the concentrations of our model input species, the distributions of which may be very sensitive to vertical transport. The diurnal variation of solar radiation will impose the tightest constraint on this assumption, as we will see below.

Ideally, the photochemical equilibrium assumption should be invoked only when the lifetime of the species or group of species under consideration is substantially below a day. This is true for many species, primarily free radical intermediate species, as may be seen in Figure 11, in which species lifetimes are plotted as a function of altitude for 35°N. This is a strong restriction for other species, however, most notably longer-lived closed shell molecules in the lower stratosphere. The lifetime of HNO_3 is over a day below approximately 15 mbar throughout the stratosphere (and below 10 mbar near the poles), for example. This suggests at first glance that method B, in which HNO_3 is assumed to be in photochemical equilibrium, should not be applied below those levels. We note that *Pyle et al.* [1983] present results down to 25 km (approximately 25 mbar). Similarly, HO_x has a lifetime of more than a day everywhere below approximately 20 km (about 50 mbar), as may be seen in Figure 12. This suggests that the sources and sinks method used here and previously [*Jackman et al.*, 1985] should not be applied below that level.

Adherence to this strict standard would mean that one could not use the LIMS data to simply infer daytime concentrations of HO_x species in the lowest 10–15 km of the stratosphere, the region of the atmosphere for which measurements are most needed. We will demonstrate that one need not adhere to such a strict standard for inferring zonally averaged concentrations of HO_x species, however.

As a way of assessing the magnitude of the error associated with the assumption of photochemical equilibrium for HO_x, HO_2NO_2, and H_2O_2 in the middle and lower stratosphere, we may consider a limited set of chemical reactions responsible for the bulk of stratospheric chemistry using the square-wave diurnal averaging framework of *Turco and Whitten* [1978]. If we assume that the concentrations of HO, HO_2, and $O(^1D)$ go to zero at night and those of H_2O_2, HO_2NO_2, HNO_3, and H_2O, as well as temperature, have equal daytime and nighttime concentrations [*Turco and Whitten*, 1978; *Fabian et al.*, 1982], we may show (see Appendix C) that the use of a photochemical equilibrium assumption for daytime HO_x, HO_2NO_2, and H_2O_2 (computed using daytime values for all other species) is substantially equivalent to the assumption of photochemical equilibrium for the diurnally averaged concentration of those species. This is a looser constraint, as the day-to-day variation in the diurnally averaged concentration will be far smaller than the diurnal variation of the same species. The latter is a reasonable assumption through most of the middle and lower stratosphere, where large changes in the zonally averaged values of the concentrations of their precursors or the temperature over a period of a few days are unlikely. Quantification of this error introduced by this assumption is difficult because of the lack of data on day-to-day variability of zonally averaged concentrations.

This equivalence is only approximate, of course, as the diurnal profiles of OH and HO_2 are not square waves with nighttime concentrations of zero, although in the lower stratosphere these are very reasonable assumptions. Thus an additional uncertainty in the inferred concentrations, which has not been taken into account in the calculation of total uncertainties, exists in the lower stratosphere. Note that the assumption of photochemical equilibrium for diurnally averaged concentrations may not be made for nonzonally averaged data (i.e., those from individual satellite orbits), and for those data one may not use a photochemical equilibrium method to infer HO_x species concentrations in the lower part of the stratosphere.

6. CONCLUSIONS

We have shown that LIMS data, together with a photochemical equilibrium model, may be used to infer concentrations of a variety of zonally averaged trace O_x, HO_x, and NO_x species over much of the stratosphere. In the lower stratosphere, where the photochemical equilibrium assumption for HO_x species breaks down, inferred concentrations should still be accurate to about a factor of 2 for OH and 2.5 for HO_2.

The photochemical model used is an essentially algebraic one so that sensitivity coefficients (logarithmic derivative of inferred concentrations with respect to input parameters) may be calculated. These are used with the estimated uncertainty of the input parameters (concentrations, rate constants, photolysis rates) to estimate the total uncertainties in the concentrations of the inferred species.

The major results include the following:

1. Concentrations of the reactive intermediates OH and HO_2 are comparable to previous measurements and model estimates.

2. Uncertainty factors for HO_x species are essentially always greater than 1.5 (approximately 50% uncertainty), with uncertainties greatest in the lower stratosphere.

3. Uncertainty factors for different species vary from one to the next. In general, $u_{H_2O_2} > u_{HO_2NO_2} > u_{HO_2} > u_{OH}$.

4. The uncertainty factors obtained may vary substantially depending on the inference procedure used. In particular, while OH calculated from the scheme used by *Pyle et al.* [1983] based on the HNO_3/NO_2 ratio is only somewhat less certain than that inferred from a version of the scheme based on HO_x sources and sinks [*Jackman et al.*, 1985], the difference is much larger for HO_2 and H_2O_2.

5. The sensitivity coefficients calculated help to elucidate which inferred concentrations are most sensitive to given model input parameters. Besides being of interest in its own right, this sensitivity may be useful in planning future measurements of model input parameters (photolysis rates, reaction rates, concentrations).

Because of the broad spatial and temporal coverage of the LIMS data, it is believed that they should be of great use in understanding the global distribution of trace species in the stratosphere, as well as their spatial and temporal variability. The total uncertainty factors derived here may prove to be especially useful in assessing measurements of concentration or reactive intermediates and long-lived trace species in the stratosphere, as they provide some indication as to how large the "error bars" on the predicted values may be. The impending development of improved and more comprehensive satellite-based remote sensing measurements (UARS, for example) suggests that this approach should be a fruitful one in the future.

APPENDIX A

The following expressions were used in the algebraic model where the LIMS HNO_3 values were used. All three-body reactions with rates t_j are written in a pseudo-bimolecular form with units of cm^3 $molecule^{-1}$ s^{-1}, so no explicit pressure dependence is indicated.

$$[O] = \frac{(J_2 + J_4)[O_3] + 2J_1[O_2]}{[O_2](t_1[N_2] + t_{12}[O_2])} \quad \text{(A1)}$$

$$[O(^1D)] = \frac{J_4[O_3]}{k_1[N_2] + k_{38}[O_2]} \quad \text{(A2)}$$

$$[O_2(^1\Delta)] = \frac{J_4[O_3]}{k_{37}[O_2]} \quad \text{(A3)}$$

$$[NO] = \frac{(J_3 + k_2[O])[NO_2]}{k_3[O_3] + (k_{28}[HO_2] + t_2[O] + J_5)} \quad \text{(A4)}$$

where the terms in parentheses in the denominator were not included in the initial estimate of [NO].

$$[OH] = \frac{-w + (w^2 + 8xv)^{1/2}}{4v} \quad \text{(A5)}$$

where x, v, and w have been given previously (e.g., equations (13*a*), (15), and (16)) but are repeated here for completeness.

$$v = k_{14}E/D + k_{34} \quad \text{(A6)}$$

$$w = 2(k_{15}[HNO_3] + k_{39}[HO_2NO_2]) \quad \text{(A7)}$$

$$x = 2\{(J_{13} + k_6[O(^1D)])[H_2O] + k_7[O(^1D)][CH_4] + k_{20}[O(^1D)][H_2] + (J_{12} + k_{25}[O])[CH_2O]\} \quad \text{(A8)}$$

$$D = k_{10}[O_3] + k_{28}[NO] + k_{11}[O] + t_8[NO_2] \quad \text{(A9)}$$

$$E = k_8[O_3] + c_1t_3[O_2]/c_2 + k_{24}v[CH_4] \quad \text{(A10)}$$

$$v = \frac{k_{32}t_7}{(k_{32} + k_{36})(t_7 + k_{35})} \quad \text{(A11)}$$

$$c_1 = k_9[O] + (k_{30} + t_{13})[CO] + k_{21}[H_2] \quad \text{(A12)}$$

$$c_2 = t_3[O_2] + k_{12}[O_3] \quad \text{(A13)}$$

and

$$[H] = (c_1[OH] + J_{12}[CH_2O] + J_{13}[H_2O] + k_{20}[O(^1D)][H_2])/c_2 \quad \text{(A14)}$$

$$[HO_2] = (k_8[O_3][OH] + t_3[H][O_2] + k_{24}v[OH][CH_4] + J_{15}[HO_2NO_2])/D \quad \text{(A15)}$$

In some cases the approximation $[HO_2] \sim E[OH]/D$ was used.

The physical significance of the terms c_1 and c_2 is that c_1 represents processes leading to OH-H conversion, while c_2 represents loss processes for H. The terms in D represent loss processes for HO_2, while E represents those processes responsible for conversion (either direct or through H) from OH to HO_2. The term v represents a product of branching ratios and represents the fraction of CH_4 oxidation events via k_{24}, which will lead to OH-HO_2 interconversion via CH_3O and CH_3O_2.

$$[CH_2O] = \frac{\{(k_7 + k_{23})[O(^1D)] + k_{24}[OH] + k_{22}[O]\}[CH_4]}{J_{11} + J_{12} + k_{25}[O] + k_{31}[OH]} \quad \text{(A16)}$$

$$[HO_2NO_2] = \frac{t_8[HO_2][NO_2]}{J_{15} + J_{16} + k_{39}[OH]} \quad \text{(A17)}$$

$$[H_2O_2] = \frac{(k_{13} + t_{11})[HO_2]^2 + t_{10}[OH]^2}{J_9 + k_{29}[OH]} \quad \text{(A18)}$$

$$[CH_3] = \frac{\{k_7[O(^1D)] + k_{24}[OH] + k_{22}[O]\}[CH_4]}{(t_7 + k_{35})[O_2]} \quad \text{(A19)}$$

$$[CH_3O_2] = \frac{t_7[CH_3][O_2]}{(k_{32} + k_{36})[NO]} \quad \text{(A20)}$$

$$[CH_3O] = \frac{t_7k_{32}[CH_3]}{(k_{32} + k_{36})k_{33}} \quad \text{(A21)}$$

$$[HCO] = \frac{J_{11} + (k_{25}[O] + k_{31}[OH])[CH_2O]}{k_{27}[O_2]} \quad \text{(A22)}$$

$$[N] = \frac{J_5[NO] + J_{14}[N_2O]}{k_4[O_2] + k_5[NO]} \quad \text{(A23)}$$

$$[N_2O_5] = \frac{-B_1A_{21}}{A_{12}A_{21} - A_{11}A_{12}} \quad \text{(A24)}$$

$$[NO_3] = A_{22}[N_2O_5]/A_{21} \quad \text{(A25)}$$

where

$$A_{11} = J_7 + J_8 + k_{17}[NO] + t_5[NO_2] + k_{40}[O] \quad \text{(A26)}$$

$$A_{12} = J_{10} + t_6 \quad \text{(A27)}$$

$$A_{21} = t_5[NO_2] \quad \text{(A28)}$$

$$A_{22} = J_{10} + t_6 + k_{18}[H_2O] + k_{19}[O] \quad \text{(A29)}$$

$$B_1 = k_{16}[NO_2][O_3] + t_9[O][NO_2] + k_{15}[OH][HNO_3] + J_{16}[HO_2NO_2] \quad \text{(A30)}$$

Where the LIMS HNO_3 values were not used, $[HNO_3]$ was solved for simultaneously with [OH]. This required the replacement of v and w in equation (A5) with the altered quantities v' and w', given by

$$v' = v + \frac{t_4 k_{15}[NO_2]}{J_6 + k_{15}[OH]} \quad \text{(A15')}$$

$$w' = w - 2k_{15}[HNO_3] \quad \text{(A16')}$$

where

$$[HNO_3] = \frac{t_4[OH][NO_2]}{J_6 + k_{15}[OH]} \quad \text{(A31)}$$

When LIMS HNO_3 values were not used, HNO_3 was thus included in the iteration loop along with OH, H, HO_2, CH_2O, and HO_2NO_2.

APPENDIX B: VALIDATION OF THE MODEL

In this appendix we will consider the question of how well the approximate equations presented in Appendix A represent the chemistry of the stratosphere. We will focus our attention on mid-latitudes (35°N), considering the pressure levels of the model centered at 90.3, 16.4, and 2.98 mbar (approximately 17, 28, and 40 km, respectively), corresponding to the lower, middle, and upper stratosphere levels examined in Tables 5–8. Our aim here is to show to what extent the chemistry scheme is complete and what approximations made are expected to place the most severe constraints on the applicability of the model. In examining this question, we will assume that our model is sufficiently accurate that we may check for completeness by using model-derived concentrations and seeing whether neglected processes might have a large effect on the concentrations inferred from a more complete model.

This validation process will be done in two steps. First, we will examine the approximations made in deriving the simplified equations given the reactions and photolysis processes included Tables 2–4, along with a few other possible reactions involving O_x, HO_x, and NO_x species. Next, we will examine the effect of the neglect of chlorine in some detail, concentrating on the HO_x species considered in this work. We will also compare our equations to the steady state equations for stratospheric constituents obtained by neglecting time derivatives in the constituent time evolution equations in chapter 5 of *Brasseur and Solomon* [1984] (hereafter referred to as BS).

In deriving equation (A1) for the steady state concentration of O, we have considered production of O by photolysis of O_2 and O_3 and its loss by recombination with O_2 to form O_3. This leads to an expression which is equivalent to equation 5.28 of BS. The accuracy of this expression may be seen in Table B1, in which we show the fraction of O production and loss accounted for by the indicated neglected terms at the three pressure levels indicated above at 35°N. Similarly, our equation (A2) for $[O(^1D)]$ is equivalent to equation 5.26 of BS and equation (4) of *Allen et al.* [1984]. The magnitude of neglected loss terms for $O(^1D)$ may also be seen in Table B1. It is clear that equation (A2) will be extremely accurate (better than 99%) for all altitudes and latitudes.

Equation (A3) for $[O_2(^1\Delta)]$ assumes production only by J_4 and removal by collision with O_2. This expression differs from the corresponding one (equation 5.20) of BS in that they include spontaneous emission from $O_2(^1\Delta)$ at 1.27μ. The radiative lifetime of $O_2(^1\Delta)$ is sufficiently long (3900 s) [*Bates*, 1982] that at the pressures of the stratosphere, loss by quenching will be at least an order of magnitude faster than loss by spontaneous emission.

We assume NO to be produced only from NO_2 via photolysis and reaction with O, while it is lost by four processes. We also perform one iteration as indicated in Appendix A and in Figure 2, the purpose of which is to allow the NO concentration to reflect the relatively large (>0.1 ppbv) concentration of HO_2 in the upper stratosphere. Equation (A3) is similar to the corresponding equation (5.147) of BS, except that they include NO loss by reaction with ClO and CH_3O_2 but do not include loss by photolysis and recombination to form NO_2.

The magnitudes of neglected production and loss processes for NO are indicated in Table B1. It is obvious that the production and loss terms are very well represented. The NO + O_3 reaction constitutes the overwhelming loss process for NO throughout the stratosphere in this model, so additional iterations of NO and HO_x are not necessary, as expected changes are at most of the order of several percent.

Among the most crucial expressions entering into the model are those for the production and loss of odd hydrogen (equations (13) of the text). These expressions are not directly comparable to those of other workers. *Park and London* [1974] considered only oxygen and hydrogen containing species in their model. For the 50–80 km region of the atmosphere their only odd hydrogen production source was H_2O via photolysis and reaction with $O(^1D)$. They also considered the HO_2 disproportionation reaction (R13) an odd hydrogen loss process and included the loss process $H + HO_2 \rightarrow H_2 + O_2$ which we have neglected. Similarly, BS (their equation 5.98) only considered the sum [H] + [OH] + $[HO_2]$ and thus considered processes forming and removing H_2O_2 as sink and source reactions, respectively. Among their source reactions they included ones corresponding to our k_6, k_7, k_{20}, and J_{13}. Thus the odd hydrogen source term used here (equation (13*a*)) is an extremely comprehensive one. Neglected terms (not counting those including chlorine), such as (R18) and (R22), were found to constitute less than 0.11% of the total odd hydrogen production at the three pressure levels examined here. The relative importance of various odd hydrogen production terms is shown in Table B2.

The odd hydrogen loss equation (equation (13*b*)) should be fairly complete also. The major neglected process is that of OH with H_2O_2 (R29). The reactions of H with HO_2 to form either $H_2 + O_2$ or $H_2O + O$ and of OH with CH_3OOH (produced by the reaction of CH_3O_2 with HO_2) have also been neglected. The relative importance of these reactions is shown in Table B2, in which we use the branching ratio for odd hydrogen loss of 0.13 obtained by *Sridharan et al.* [1982] for the $H + HO_2$ reaction and the recommended total reaction rate [*DeMore et al.*, 1983] of 7.4×10^{-11} cm^3 molecule^{-1} s^{-1}. We assume the production of CH_3OOH to be entirely due to the reaction of CH_3O_2 with HO_2 at the recommended rate [*DeMore et al.*, 1983] of 7.7×10^{-14} exp (300/T) cm^3 molecule^{-1} s^{-1}. We further assume, as suggested by BS, that it is lost only by reaction with OH, occurring at a rate [*DeMore et al.*, 1983] of 10^{-11} cm^3 molecule^{-1} s^{-1}. In deriving the concentrations of CH_3OOH used in preparing Table B2, we assumed that the reaction of CH_3OOH with HO_2, not

TABLE B1. Fraction of Species Production and Loss Accounted for by Model Expressions at 35°N

Processes	Included Reactions	Neglected Reactions	Pressure, mbar	F_N[a]
O production	$O_3 + h\nu \rightarrow$ products	$NO_2 + h\nu \rightarrow NO + O$	90	7.05(−3)
	$O_2 + h\nu \rightarrow 2O$	$O(^1D) + O_3 \rightarrow O_2 + 2O$	16	7.59(−3)
		$NO_3 + h\nu \rightarrow NO_2 + O$	3	1.5(−3)
		$2OH \rightarrow H_2O + O$		
		$NO + h\nu \rightarrow N + O$		
		$NO + O_2 \rightarrow NO_2 + O$		
		$N_2O + h\nu \rightarrow N_2 + O(^1D)$		
O loss	$O + O_2 + N_2 \rightarrow O_3 + N_2$	$O + NO_2 \rightarrow NO + O_2$	90	6.60(−6)
	$O + O_2 + O_2 \rightarrow O_3 + O_2$	$O + O_3 \rightarrow 2O_2$	16	4.08(−4)
		$O + HO_2 \rightarrow OH + O_2$	3	5.04(−3)
		$O + OH \rightarrow O_2 + H$		
		$O + NO + M \rightarrow NO_2 + M$		
$O(^1D)$ loss	$O(^1D) + N_2 \rightarrow O + N_2$	$O(^1D) + O_3 \rightarrow$ products	90	3.45(−5)
	$O(^1D) + O_2 \rightarrow O + O_2$	$O(^1D) + H_2O \rightarrow 2OH$	16	9.78(−5)
		$O(^1D) + CH_4 \rightarrow$ products	3	1.02(−4)
		$O(^1D) + H_2 \rightarrow OH + H$		
NO production	$NO_2 + h\nu \rightarrow NO + O$	$NO_3 + h\nu \rightarrow NO + O_2$	90	1.45(−4)
	$O + NO_2 \rightarrow NO + O_2$	$N + O_2 \rightarrow NO + O$	16	3.77(−4)
		$N_2O + h\nu \rightarrow N + NO$	3	2.97(−4)
NO loss	$NO + O_3 \rightarrow NO_2 + O$	$CH_3O_2 + NO \rightarrow$ products	90	1.63(−4)
	$HO_2 + NO \rightarrow OH + NO_2$		16	2.96(−4)
	$O + NO + M \rightarrow NO_2 + M$		3	1.71(−3)
	$NO + h\nu \rightarrow N + O$			

[a]Read 7.05(−3) as 7.05×10^{-3}.

included in our model, is not an appreciable loss process for CH_3O_2. This fact, coupled with the neglect of other processes removing CH_3OOH, means that the HO_x loss due to CH_3OOH presented in Table B2 should represent an upper limit to the actual value. Clearly, these neglected terms should not amount to more than 3% of the odd hydrogen loss in the stratosphere, with the $H + HO_2$ reaction contributing near the 0.1% level only in the very topmost part of the stratosphere.

The treatment of processes responsible for the interconversion of H, OH, and HO_2 are very well represented in our model. The only such process included in the HO_x section of the JPL report [*DeMore et al.*, 1983] not included in equations (A15)–(A25) is the reaction of OH with H_2O_2 (k_{29}). The rate of this reaction is at most 0.2% of the rate of the reaction of OH with O_3 (the major process converting OH to HO_2) over the region of the atmosphere studied here. All other processes indicated by BS in their Figure 5.26 are included in our model.

Our expression for CH_2O (equation (A16)) included all terms included by BS in their equation 5.62 with the exception, of course, of terms involving Cl (which occur both in their numerator and denominator). In addition, we included the reaction of O with CH_4 (k_{22}) in the numerator. Similarly, our expression for HO_2NO_2 is identical to their equation 5.141 except for our neglect of thermal dissociation. It has

TABLE B2. Fractional Contributions to HO_x Loss and Production Rates at 35°N

	Pressure Level		
	90 mbar	16 mbar	3 mbar
Production process			
$O(^1D) + H_2O \rightarrow 2OH$	4.35(−1)	6.55(−1)	7.55(−1)
$H_2O + h\nu \rightarrow H + OH$	3.43(−3)	5.53(−2)	8.32(−2)
$O(^1D) + CH_4 \rightarrow OH + CH_3$	1.65(−1)	1.12(−1)	5.70(−2)
$Cl + CH_4 \rightarrow HCl + CH_3$	8.21(−2)	4.87(−2)	3.25(−2)
$O + CH_2O \rightarrow OH + HCO$	1.24(−4)	2.49(−3)	2.29(−2)
$CH_2O + h\nu \rightarrow H + HCO$	2.71(−1)	8.02(−2)	2.02(−2)
$O(^1D) + H_2 \rightarrow OH + H$	4.05(−2)	3.32(−2)	1.42(−2)
$Cl + CH_2O \rightarrow HCl + CHO$	1.80(−3)	1.30(−2)	1.33(−2)
$O + CH_4 \rightarrow OH + CH_3$	1.90(−5)	8.98(−5)	7.53(−4)
$N_2O_5 + H_2O \rightarrow 2HNO_3$	5.46(−5)	2.92(−6)	1.28(−10)
Loss			
$OH + HO_2 \rightarrow H_2O + O_2$	2.47(−2)	3.33(−1)	8.85(−1)
$OH + HCl \rightarrow H_2O + Cl$	1.02(−1)	6.01(−2)	6.54(−2)
$OH + OH \rightarrow H_2O + O$	1.27(−4)	1.36(−3)	2.75(−2)
$OH + H_2O_2 \rightarrow H_2O + HO_2$	4.33(−4)	2.40(−2)	1.14(−2)
$OH + CH_3OOH \rightarrow H_2O + CH_3O_2$	3.83(−3)	1.38(−2)	5.94(−3)
$OH + HNO_3 \rightarrow H_2O + NO_3$	4.67(−1)	1.54(−1)	3.31(−3)
$OH + HO_2NO_2 \rightarrow H_2O + NO_2 + O_2$	4.01(−1)	4.13(−1)	1.81(−3)
$H + HO_2 \rightarrow H_2 + O_2$, $H_2O + O$	1.32(−10)	3.58(−8)	3.72(−5)

Read 4.35(−1) as 4.35×10^{-1}.

been previously established [*DeMore et al.*, 1983] that this is unimportant in the stratosphere. Equation (A18) for H_2O_2 also includes all terms present in the corresponding equation of BS (equation 5.108), as well as an additional term coming from the three-body recombination of OH, which is not expected to be especially important. We note that we have neglected reactions of O with H_2O_2 and HO_2NO_2 for which rate recommendations exist [*DeMore et al.*, 1983], as their large activation energies (4 and 6.7 kcal/mol, respectively) will make them unimportant at the low temperatures of the stratosphere.

Our treatment of the intermediates (CH_3, CH_3O_2, and CH_3O) in CH_4 oxidation is in general less complete than that of BS (see their equations 5.56–5.58) due to our neglect of CH_3OOH, the self-reaction of CH_3O_2, and the reaction of CH_3O_2 with NO_2. Less than 5% of the CH_3O_2 formed is transformed to CH_3OOH; the rest goes on to form CH_3O or CH_2O by k_{32} and k_{36}, respectively. Self-reaction of CH_3O_2 should remove at most 0.1% of the CH_3O_2. The reaction of CH_3O_2 with NO_2 included by BS (which leads to formation of CH_2O and HNO_3) is in their view unimportant. Thus the scheme used here for CH_3O_2 chemistry is probably accurate to the 95% level. The neglect of CH_3OOH and of the CH_3O_2 self-reaction are responsible for our equation (A21) being much simpler than the steady state version of BS equation 5.58. Our expression for HCO (equation (A22)) is comparable to that of BS (their equation 5.61) except for their inclusion of HCO photolysis and of its production by the reaction of Cl with CH_2O, which we have not included.

The expression we presented for N is very similar to the corresponding expression (equation 5.166) of BS, except that we do not include the ionic production terms which they needed for their expression to be valid in the mesosphere. We also include a minor channel for production by photolysis of N_2O (J_{14}).

The expressions for daytime NO_3 and N_2O_5 include all reactions involving these species used by BS (their equations 5.139 and 5.140) and several additional ones. Our expressions, which assume photochemical equilibrium, should yield accurate values for daytime NO_3 concentrations, as the photochemical lifetime of NO_3 is extremely short (see Figure 11). Indeed the altitude profile of NO_3 inferred from our model is qualitatively similar and of the same magnitude as the noon profile of *Fabian et al.* [1982] for summer. For N_2O_5, however, our model is expected to be accurate only for those altitudes where the photochemical lifetime of N_2O_5 is substantially below a day. If we restrict our consideration of N_2O_5 to pressure levels where over 6 hours (half of a 12-hour day at equinox) of photolysis will remove 90% of the N_2O_5, we should only use our computed N_2O_5 values where its photolysis rate exceeds 10^{-4} s^{-1} (approximately 35 km). Comparison of our inferred noontime N_2O_5 concentrations with those from the time-dependent model of *Fabian et al.* [1982] shows that our model adequately (to within approximately a factor of 2) represents daytime N_2O_5 above this level, where its concentration does not exceed 5–10 pptv.

The major assumption remaining in the model which has yet to be treated in detail is that of neglecting chlorine. The inclusion of chlorine is expected to affect our results in several ways. First, Cl alters the NO-NO_2 partitioning by the reaction

$$ClO + NO \rightarrow Cl + NO_2 \quad (B1)$$

It may also interact with NO_2 leading to the formation of $ClONO_2$:

$$ClO + NO_2 + M \rightarrow ClONO_2 + M \quad (B2)$$

although this latter process should not be important here where NO_2 is given by the LIMS observations. Second, Cl may alter the OH-HO_2 balance by processes such as

$$HO_2 + ClO \rightarrow HOCl + O_2 \quad (B3)$$

$$HOCl + h\nu \rightarrow Cl + OH \quad (B4)$$

$$Cl + HO_2 \rightarrow ClO + OH \quad (B5)$$

Third, Cl may affect the production and loss of odd hydrogen by the reactions

$$Cl + CH_4 \rightarrow HCl + CH_3 \quad (B6)$$

$$Cl + CH_2O \rightarrow HCl + CHO \quad (B7)$$

$$OH + HCl \rightarrow H_2O + Cl \quad (B8)$$

where we now consider HCl to be an additional odd hydrogen species. We will consider each of these possible roles of chlorine separately.

The neglect of chlorine means that reaction (B1), a significant loss process for NO is being missed, so that the inferred NO concentration will exceed the true one. Using the mean of the observed ClO profiles from 25 to 40 km [*WMO*, 1982] and a model-derived ClO profile from 40 to 46 km [*Ko and Sze*, 1984], we estimate the overcalculation of mid-latitude NO to exceed 10% from 35 to 45 km, reaching a maximum of 25% at 40 km. This region of moderate error is localized to a relatively narrow altitude band because below 35 km the overwhelming NO removal process is reaction with O_3 (k_3), while above 40 km, the ClO concentration is believed to decrease rapidly with increasing altitude [*Ko and Sze*, 1984]. This error in inferring the concentration of NO should only have an appreciable effect on the HO_x species concentrations at those altitudes where the major process responsible for HO_2-OH conversion is the reaction of HO_2 with NO (k_{28}). This is true below approximately 32 km; above 40 km the reaction of HO_2 with O (k_{11}) is responsible for more than 90% of the HO_2-OH conversion. Recall that at the 40-km level the expected error in NO is of the order of 25%. Thus, errors in HO_2 and OH concentrations due to the neglect of Cl will be related to the product of two fractional errors. At mid-latitudes this error does not exceed 5%, and it should not be appreciably greater (more than a factor of 2) at other latitudes.

The effect of Cl on HO_2-OH interconversion by other processes is also expected to be small. Assuming all HOCl produced by reaction (B3) is photolyzed to Cl + OH, we have estimated HO_2-OH conversion via processes (B3) and (B4) to be no more than 2% of the total. The fraction occurring by equation (B5) will be even smaller due to the low concentrations of Cl expected in the stratosphere and the rough equivalence of the rate constants for reactions (B3) and (B5).

Finally, the effect of chlorine chemistry on odd hydrogen production and loss is expected to be small. We have compared the magnitude of odd hydrogen production expected due to reactions (B6) and (B7) using Cl mixing ratios of 10^{-15}, 10^{-13}, and 10^{-11} (somewhat above the values estimated from Figure 5.57 of BS) at our lower, middle, and upper stratosphere levels, respectively, to the total odd hydrogen production rate from processes included in our model. These values are included in Table B2. The largest contribution from Cl (10%) occurs in the lower stratosphere, with the predominant contribution there coming from reaction (B5). Similarly, the contribution of reaction (B8) to the total odd hydrogen

TABLE B3. Fractional Contributions to CH_2O Loss and Production Rates at 35°N

	Pressure Level		
	90 mbar	16 mbar	3 mbar
Production CH_4 destruction			
$OH + CH_4 \rightarrow H_2O + CH_3$	0.751	0.550	0.518
$O(^1D) + CH_4 \rightarrow$ products	0.166	0.316	0.305
$Cl + CH_4 \rightarrow HCl + CH_3$	8.30(−2)	0.137	0.174
$O + CH_4 \rightarrow OH + CH_3$	1.92(−5)	2.53(−4)	4.03(−3)
Loss			
$OH + CH_2O \rightarrow H_2O + CHO$	5.50(−2)	0.271	0.506
$CH_2O + h\nu \rightarrow$ products	0.942	0.698	0.260
$O + CH_2O \rightarrow$ products	1.32(−3)	7.65(−3)	0.127
$Cl + CH_2O \rightarrow HCl + CHO$	2.21(−3)	2.29(−2)	0.106

Read 8.30(−2) as 8.30×10^{-2}.

loss was estimated using HCl mixing ratios of 0.5, 1.25, and 2.5 ppbv (also estimated from Figure 5.57 of BS) and was found to amount to between 6 and 12% of the total. The values calculated are shown in Table B2. Again, the largest contribution was in the lower stratosphere.

The neglect of chlorine should not have a major effect on the other inferred species. The largest effect is expected for the methane oxidation products, of which CH_2O is of most interest, as it is the only one to reach concentrations greater than 0.1 ppbv. As noted earlier, Cl leads both to production (via reaction (B6)) and destruction (from reaction (B7)) of CH_2O. A comparison of the various production and loss terms for CH_2O showing the relative magnitude of the chlorine terms is given in Table B3. It is apparent that inclusion of chlorine would lead to enhanced CH_2O concentrations by amounts which should not exceed 10% throughout the stratosphere. Chlorine is also expected to react with H_2O_2 [*DeMore et al.*, 1983] and HO_2NO_2 [*Simonaitis and Leu*, 1985], but these reactions are sufficiently slow as to be negligible.

APPENDIX C

We will use the formalism of *Turco and Whitten* [1978] to demonstrate the approximate equivalence of the assumption of photochemical equilibrium assumptions for both daytime and diurnally averaged HO_x, HO_2NO_2, and H_2O_2. We assume that at night the concentrations of OH, HO_2, and $O(^1D)$ are all zero, while those of HNO_3, HO_2NO_2, and H_2O are unchanged from their daytime values.

For a very simplified model of the HO_x chemistry of the middle and lower stratosphere, we approximate equations (13*a*) and (13*b*) of the text by (using the subscript "av" to represent diurnal averages).

$$P(HO_x) = 2\beta_{k_6} k_6 [O(^1D)]_{av}[H_2O]_{av} \quad \text{(C1)}$$

TABLE C1. Constants for *Turco and Whitten* [1978] Analysis

Species	r_1[a]	α_1[b]
OH	0	f
HO_2	0	f
$O(^1D)$	0	f
H_2O	1	1
HNO_3	1	1
H_2O_2	1	1
HO_2NO_2	1	1
NO_2	g	$f + (1-f)g$

[a] r_1, nighttime concentration/daytime concentration.
[b] $\alpha_i = f + r_i(1-f)$; f, fraction of day with daylight.

TABLE C2. β Parameters for *Turco and Whitten* [1978] Analysis

Process	Species i	α_i	Species j	α_j	β_{ij}
k_6	$O(^1D)$	f	H_2O	1	1
k_{14}	OH	f	NO_2	f	$1/f$
k_{15}	OH	f	HNO_3	1	1
k_{39}	OH	f	HO_2NO_2	1	1
J_{15}	HO_2NO_2	1	...	...	f
J_{16}	HO_2NO_2	1	...	...	f
t_8	HO_2	f	NO_2	$f + g(1-f)$	$1/[f + g(1-f)]$
J_9	H_2O_2	1	...	...	f
k_{29}	OH	f	H_2O_2	1	1
k_{11}	HO_2	f	HO_2	f	$1/f$

$\beta_{ij} = 1 + [f/(1-f)](1-\alpha_j^{-1})(1-\alpha_k^{-1})$ for chemical reactions and equals f for photolysis processes.

$$L(HO_x) = 2[OH]_{av}(\beta_{k_{14}} k_{14}[HO_2]_{av} + \beta_{k_{15}} k_{15}[HNO_3]_{av} + \beta_{k_{39}} k_{39}[HO_2NO_2]_{av}) \quad \text{(C2)}$$

where β_i are the correction factors defined by equation 14 of *Turco and Whitten* [1978]. The day-night concentration ratios assumed are shown in Table C1, and the β values used are shown in Table C2. From equations (1) and Tables C1 and C2 we see that

$$2k_6[O(^1D)]_{av}[H_2O]_{av} = 2[OH]_{av}(k_{14}[HO_2]_{av}/f + k_{15}[HNO_3]_{av} + k_{39}[HO_2NO_2]_{av}) \quad \text{(C3)}$$

Equation (B3) may be rewritten in terms of daytime concentrations by use of equation 12 of *Turco and Whitten* [1978] and our assumptions to give

$$2fk_6[O(^1D)]_d[H_2O]_d = 2f[OH]_d(k_{14}[HO_2]_d + k_{15}[HNO_3]_d + k_{39}[HO_2NO_2]_d) \quad \text{(C4)}$$

where the subscript "d" is used to indicate daytime concentrations and f is the fraction of day with daylight. Clearly, unless $f = 0$, equation (B4) is exactly equivalent to the use of a photochemical equilibrium assumption for daytime HO_x, as was made throughout this paper.

For HO_2NO_2, we replace equation (17) by

$$(\beta_{J_{15}} J_{15} + \beta_{J_{16}} J_{16} + \beta_{k_{39}} k_{39}[OH]_{av})[HO_2NO_2]_{av} = \beta_{t_8} t_8 [HO_2]_{av}[NO_2]_{av}$$

which, using the β values in Table B2, gives

$$(fJ_{15} + fJ_{16} + k_{39}[OH]_{av})[HO_2NO_2]_{av} = \frac{1}{f + g(1-f)} t_8 [HO_2]_{av}[NO_2]_{av}$$

and on changing to daytime concentrations gives

$$f(J_{15} + J_{16} + k_{39}[OH]_d)[HO_2NO_2]_d = ft_8[HO_2]_d[NO_2]_d$$

which again is equivalent to what would be obtained with an assumption of daytime photochemical equilibrium.

Similarly, for H_2O_2, one may show that

$$(\beta_{J_9} J_9 + \beta_{k_{29}} k_{29}[OH]_{av})[H_2O_2]_{av} = \beta_{k_{13}} k_{13}[HO_2]_{av}^2$$

or

$$(fJ_9 + k_{29}[OH]_{av})[H_2O_2]_{av} = \frac{1}{f} k_{13}[HO_2]_{av}^2$$

so

$$f(J_9 + k_{29}[OH]_d)[H_2O_2]_d = fk_{13}[HO_2]_d^2$$

which also is equivalent to a daytime photochemical equilibrium assumption.

Acknowledgments. We thank J. R. Herman and C. J. McQuillan for assistance in using their one-dimensional model to help validate the approximation scheme used. We thank R. Stolarski and M. Geller for helpful discussions and their encouragement of this work. We also thank J. A. Pyle for sending us a preprint of Pyle and Zavody (1985). We are grateful to Roberta M. Duffy for her assistance in the preparation of this manuscript. Contribution 26 of the Stratospheric General Circulation with Chemistry Modeling Project at NASA Goddard Space Flight Center.

REFERENCES

Allen, M., J. L. Lunine, and Y. L. Yung, The vertical distribution of ozone in the mesosphere and lower thermosphere, *J. Geophys. Res.*, *89*, 4841–4872, 1984. (Correction, *J. Geophys. Res.*, *89*, 11827, 1984.)

Anderson, J. G., H. J. Grassl, R. E. Shetter, and J. J. Margitan, HO_2 in the stratosphere: Three in situ observations, *Geophys. Res. Lett.*, *8*, 289–292, 1981.

Barnett, J. J., M. Corney, A. K. Murphy, R. L. Jones, C. D. Rodgers, F. W. Taylor, E. J. Williams, and N. M. Vyas, Global and seasonal variability of the temperature and composition of the middle atmosphere, *Nature*, *313*, 438–443, 1985.

Bates, D. R., Airglow and auroras, in *Applied Atomic Collision Physics*, vol. 1, p. 176, Academic, Orlando, Fla., 1982.

Berg, W. W., P. J. Crutzen, F. E. Grahek, S. N. Gitlin, and W. A. Sedlacek, First measurements of total chlorine in the lower stratosphere, *Geophys. Res. Lett.*, *7*, 937–940, 1980.

Brasseur, G., and S. Solomon, *Aeronomy of the Middle Atmosphere*, pp. 201–319, D. Reidel, Hingham, Mass., 1984.

Butler, D. M., The uncertainty in ozone calculations by a stratospheric photochemistry model, *Geophys. Res. Lett.*, *5*, 769–772, 1978.

Butler, D. M., Input sensitivity study of a stratospheric photochemistry model, *Pure Appl. Geophys.*, *117*, 430–435, 1979.

Callis, L. B., M. Natarajan, and J. M. Russell III, Estimates of the stratospheric distribution of odd nitrogen from the LIMS data, *Geophys. Res. Lett.*, *12*, 259–262, 1985.

Cunnold, D. M., M. C. Pitts, and C. R. Trepte, An intercomparison of SAGE and SBUV zone observations for March and April 1979, *J. Geophys. Res.*, *89*, 5249–5262, 1984.

DeMore, W. B., M. J. Molina, R. T. Watson, D. M. Golden, R. F. Hampson, M. J. Kurylo, C. J. Howard, and A. K. Ravishankara, Chemical kinetics and photochemical data for use in stratospheric modeling, *JPL Publ.*, *83-62*, 1983.

Derwent, R. G., and A. E. J. Eggleton, On the validation of one-diensional CFC-ozone depletion models, *Nature*, *293*, 387–389, 1981.

de Zafra, R. L., A. Parrish, P. M. Solomon, and J. W. Barrett, A measurement of stratospheric HO_2 by ground-based millimeter wave spectroscopy, *J. Geophys. Res.*, *89*, 1321–1326, 1984.

Fabian, P., J. A. Pyle, and R. J. Wells, Diurnal variations of minor constituents in the stratosphere modeled as a function of latitude and season, *J. Geophys. Res.*, *87*, 4981–5000, 1982.

Garcia, R. R., and S. Solomon, A numerical model of the zonally averaged dynamical and chemical structure of the middle atmosphere, *J. Geophys. Res.*, *88*, 1379–1400, 1983.

Gille, J. C., and J. M. Russell III, The limb infrared monitor of the stratosphere: Experiment description, performance, and results, *J. Geophys. Res.*, *89*, 5125–5140, 1984.

Gille, J. C., J. M. Russell III, P. L. Bailey, E. E. Remsberg, L. L. Gordley, W. F. J. Evans, H. Fischer, B. W. Gandrud, A. Girard, J. E. Harries, and S. A. Beck, Accuracy and precision of the nitric acid concentration determined by the limb infrared monitor of the stratosphere experiment on Nimbus 7, *J. Geophys. Res.*, *89*, 5179–5190, 1984*a*.

Gille, J. C., J. M. Russell III, P. L. Bailey, L. L. Gordley, E. E. Remsberg, J. H. Lienesch, W. G. Planet, F. B. House, L. V. Lyjak, and S. A. Beck, Validation of temperature retrievals obtained by the limb infrared monitor of the stratosphere (LIMS) experiment on Nimbus 7, *J. Geophys. Res.*, *89*, 5147–5160, 1984*b*.

Guthrie, P. D., C. H. Jackman, J. R. Herman, and C. J. McQuillan, A diabatic circulation experiment in a two-dimensional photochemical model, *J. Geophys. Res.*, *89*, 9589–9602, 1984*a*.

Guthrie, P. D., C. H. Jackman, and A. M. Thompson, Methane and carbon monoxide: Budgets and seasonal behavior in a 2-D model simulation, *Eos Trans. AGU*, *65*, 834, 1984*b*.

Hampson, R. F., Chemical kinetic and photochemical data sheets for atmospheric reactions, *Rep. FAA-EE-80-17*, U.S. Dep. of Transport., Washington, D. C., 1980.

Hampson, R. F., and D. Garvin (Eds.), Reaction rate and photochemical data for atmospheric chemistry 1977, *NBS Spec. Publ.*, *513*, 1978.

Harries, J. E., Stratospheric composition measurements as test of photochemical theory, *J. Atmos. Terr. Phys.*, *44*, 591–597, 1982.

Herman, J. R., The response of stratospheric constituents to a solar eclipse, sunrise, and sunset, *J. Geophys. Res.*, *84*, 3701–3710, 1979.

Jackman, C. H., J. A. Kaye, and P. D. Guthrie, LIMS HNO_3 data above 5 mbar: Corrections based on simultaneous observations of other species, *J. Geophys. Res.*, *90*, 7923–7930, 1985.

Jones, R. L., Satellite measurements of atmospheric composition: three years' observations of CH_4 and N_2O, *Adv. Space Res.*, *4*, 121–130, 1984.

Jones, R. L., and J. A. Pyle, Observations of CH_4 and N_2O by the Nimbus 7 SAMS: A comparison with in situ data and two-dimensional numerical model calculations, *J. Geophys. Res.*, *89*, 5263–5279, 1984.

Ko, M. K. W., and N. D. Sze, Diurnal variations of ClO: Implications for the stratospheric chemistries of $ClONO_2$, HOCl, and HCl, J. Geophys. Res., *89*, 11619–11632, 1984.

Leovy, C. P., Atmospheric ozone: An analytic model for photochemistry in the presence of water vapor, *J. Geophys. Res.*, *74*, 417–426, 1969.

McPeters, R. D., D. F. Heath, and P. K. Bhartia, Average ozone profiles for 1979 from the Nimbus 7 SBUV instrument, *J. Geophys. Res.*, *89*, 5199–5214, 1984.

Mihelcic, D., D. H. Ehhalt, G. F. Kulessa, J. Klomfass, M. Trainer, U. Schmidt, and H. Rohrs, Measurements of free radicals in the atmosphere by matrix isolation and electron paramagnetic resonance, *Pure Appl. Geophys.*, *116*, 530–536, 1978.

Miller, C., D. L. Filkin, A. J. Owens, J. M. Steed, and J. P. Jesson, A two-dimensional model of stratospheric chemistry and transport, *J. Geophys. Res.*, *86*, 12039–12065, 1981.

Mount, G. H., D. W. Rusch, J. M. Zawodny, J. F. Noxon, C. A. Barth, G. J. Rottman, R. J. Thomas, G. E. Thomas, R. W. Sanders, and G. M. Lawrence, Measurements of NO_2 in the earth's stratosphere using a limb scanning visible light spectrometer, *Geophys. Res. Lett.*, *10*, 265–268, 1983.

Mount, G. H., D. W. Rusch, J. F. Noxon, J. M. Zawodny, and C. A. Barth, Measurements of stratospheric NO_2 from the Solar Mesosphere Explorer Satellite, 1, An overview of the results, *J. Geophys. Res.*, *89*, 1327–1340, 1984.

NASA, The stratosphere: Present and future, *NASA Ref. Publ. 1049*, 1979.

Naudet, J. P., P. Rigaud, and D. Huguenin, Stratospheric NO_2 at night from balloons, *J. Geophys. Res.*, *89*, 2583–2587, 1984.

Park, J. H., and J. London, Ozone photochemistry and radiative heating of the middle atmosphere, *J. Atmos. Sci.*, *31*, 1898–1916, 1974.

Pyle, J. A., and A. M. Zavody, The derivation of near-global fields of hydrogen-containing radical concentrations from satellite data sets, *Q. J. R. Meteorol. Soc.*, in press, 1985.

Pyle, J. A., A. M. Zavody, J. E. Harries, and P. H. Moffatt, Derivation of OH concentration from satellite infrared measurements of NO_2 and HNO_3, *Nature*, *305*, 690–692, 1983.

Pyle, J. A., A. M. Zavody, J. E. Harries, and P. H. Moffat, Derivation of OH concentrations from LIMS measurements, *Adv. Space Res.*, *4*, 117–120, 1984.

Rabitz, H., M. Kramer, and D. Dacol, Sensitivity analysis in chemical kinetics, *Annu. Rev. Phys. Chem.*, *34*, 419–463, 1983.

Remsberg, E. E., J. M. Russell III, J. C. Gille, L. L. Gordley, P. L. Bailey, W. G. Planet, and J. E. Harries, The validation of Nimbus 7 LIMS measurements of ozone, *J. Geophys. Res.*, *89*, 5161–5178, 1984.

Rodgers, C. D., R. L. Jones, and J. J. Barnett, Retrieval of temperature and composition from Nimbus 7 SAMS measurements, *J. Geophys. Res.*, *89*, 5280–5286, 1984.

Rundle, R. D., D. M. Butler, and R. S. Stolarski, Uncertainty propagation in a stratospheric model, 1, Development of a concise stratospheric model, *J. Geophys. Res.*, *83*, 3063–3073, 1978.

Russell, J. M., III, The global distribution and variability of stratospheric constituents measured by LIMS, *Adv. Space Res.*, *4*, 107–116, 1984.

Russell, J. M., III, E. E. Remsberg, L. L. Gordley, J. C. Gille, and P. L. Bailey, The variability of stratospheric nitrogen compounds observed by LIMS in the winter of 1978–1979, *Adv. Space Res.*, *2*, 169–172, 1983.

Russell, J. M., III, J. C. Gille, E. E. Remberg, L. L. Gordley, P. L.

Bailey, H. Fischer, A. Girard, S. R. Drayson, W. F. J. Evans, and J. E. Harries, Validation of water vapor results measured by the limb infrared monitor of the stratosphere experiment on Nimbus 7, *J. Geophys. Res.*, *89*, 5115–5124, 1984*a*.

Russell, J. M., III, J. C. Gille, E. E. Remsberg, L. L. Gordley, P. L. Bailey, S. R. Drayson, H. Fischer, A. Girard, J. E. Harries, and W. F. J. Evans, Validation of nitrogen dioxide results measured by the limb infrared monitor of the stratosphere (LIMS) experiment on Nimbus 7, *J. Geophys. Res.*, *89*, 5099–5107, 1984*b*.

Simonaitis, R., and M. T. Leu, Rate constant for the reaction Cl + $HO_2NO_2 \rightarrow$ products, *Int. J. Chem. Kinet.*, *17*, 293–301, 1985.

Solomon, S., and R. R. Garcia, On the distribution of nitrogen dioxide in the high-latitude stratosphere, *J. Geophys. Res.*, *88*, 5229–5239, 1983.

Spridharan, U. C., L. X. Qiu, and F. Kaufman, Kinetics and product channels of the reactions of HO_2 with O and H atoms at 296 K, *J. Phys. Chem.*, *86*, 4569–4574, 1982.

Stolarski, R. S., Uncertainty and sensitivity studies of stratospheric photochemistry, in *Proceedings of the NATO Advanced Study Institute on Atmospheric Ozone: Its Variation and Human Influences*, edited by A. C. Aikin, U.S. Department of Transportation, Federal Aviation Administration, Washington, D. C., 1980.

Thomas, R. J., C. A. Barth, D. W. Rusch, and R. W. Sanders, Solar mesosphere explorer near-infrared spectrometer: Measurements of 1.27-μm radiances and the inference of mesospheric ozone, *J. Geophys. Res.*, *89*, 9569–9580, 1984.

Turco, R. P., and R. C. Whitten, A note on the diurnal averaging of aeronomical models, *J. Atmos. Terr. Phys.*, *40*, 13–20, 1978.

World Meteorological Organization, The stratosphere 1981: Theory and measurements, *Rep. 11*, Global Ozone Res. and Monit. Proj., Geneva, Switzerland, 1982.

C. H. Jackman and J. A. Kaye, Atmospheric Chemistry and Dynamics Branch, Code 616, NASA Goddard Space Flight Center, Greenbelt, MD 20771.

(Received April 4, 1985;
revised July 29, 1985;
accepted August 1, 1985.)